AD-A153 773 DEVELOPMENT OF PHOTODETECTORS(U) RCA INC STE ANNE DE BELLEVUE (QUEBEC) R MCINTYRE ET AL. JAN 85 RADC-TR-84-217 F19628-82-C-0038 1/1

UNCLASSIFIED F/G 9/1 NL

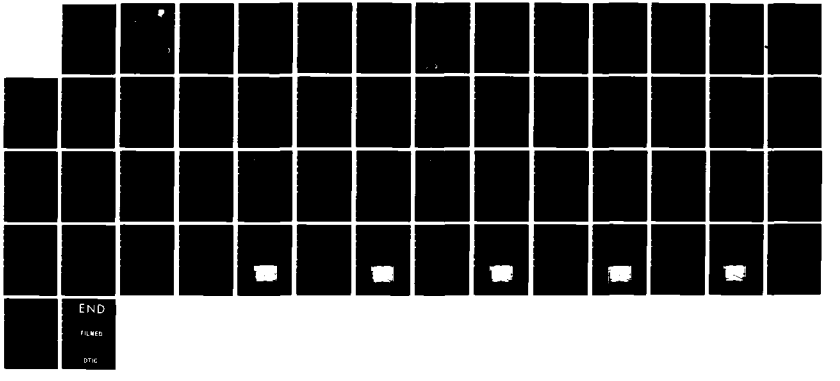

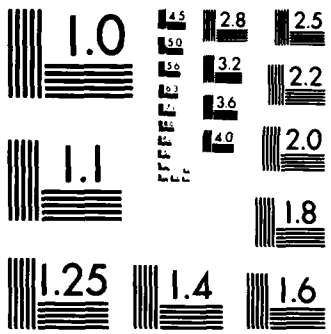

MICROCOPY RESOLUTION TEST CHART
NATIONAL BUREAU OF STANDARDS-1963-A

(2)

RADC-TR-84-217
Final Technical Report
January 1985

DEVELOPMENT OF PHOTODETECTORS

RCA Inc.

R. McIntyre
P. Webb

APPROVED FOR PUBLIC RELEASE; DISTRIBUTION UNLIMITED

ROME AIR DEVELOPMENT CENTER
Air Force Systems Command
Griffiss Air Force Base, NY 13441-5700

This report has been reviewed by the RADC Public Affairs Office (PA) and is releasable to the National Technical Information Service (NTIS). At NTIS it will be releasable to the general public, including foreign nations.

RADC-TR-84-217 has been reviewed and is approved for publication.

APPROVED: J. P. Lorenzo

JOSEPH P. LORENZO
Project Engineer

APPROVED: Harold Roth

HAROLD ROTH, Director
Solid State Sciences Division

FOR THE COMMANDER: John A. Ritz

JOHN A. RITZ
Acting Chief, Plans Office

If your address has changed or if you wish to be removed from the RADC mailing list, or if the addressee is no longer employed by your organization, please notify RADC (ESO) Hanscom AFB MA 01731. This will assist us in maintaining a current mailing list.

Do not return copies of this report unless contractual obligations or notices on a specific document requires that it be returned.

REPORT DOCUMENTATION PAGE

1a. REPORT SECURITY CLASSIFICATION UNCLASSIFIED	1b. RESTRICTIVE MARKINGS N/A
2a. SECURITY CLASSIFICATION AUTHORITY N/A	3. DISTRIBUTION/AVAILABILITY OF REPORT Approved for public release; distribution unlimited
2b. DECLASSIFICATION/DOWNGRADING SCHEDULE N/A	
4. PERFORMING ORGANIZATION REPORT NUMBER(S) N/A	5. MONITORING ORGANIZATION REPORT NUMBER(S) RADC-TR-84-217
6a. NAME OF PERFORMING ORGANIZATION RCA, Inc. — 6b. OFFICE SYMBOL (If applicable)	7a. NAME OF MONITORING ORGANIZATION Rome Air Development Center (ESO)
6c. ADDRESS (City, State and ZIP Code) Box 1200 Ste-Anne-de-Bellevue Quebec, Canada H9X 3L3	7b. ADDRESS (City, State and ZIP Code) Hanscom AFB MA 01731
8a. NAME OF FUNDING/SPONSORING ORGANIZATION Rome Air Development Center — 8b. OFFICE SYMBOL (If applicable) ESO	9. PROCUREMENT INSTRUMENT IDENTIFICATION NUMBER F19628-82-C-0038
8c. ADDRESS (City, State and ZIP Code) Hanscom AFB MA 01731	10. SOURCE OF FUNDING NOS. PROGRAM ELEMENT NO. 62702F — PROJECT NO. 4600 — TASK NO. 19 — WORK UNIT NO. 37
11. TITLE (Include Security Classification) DEVELOPMENT OF PHOTODETECTORS	
12. PERSONAL AUTHOR(S) R. McIntyre, P. Webb	
13a. TYPE OF REPORT Final	13b. TIME COVERED FROM June 83 TO June 84 — 14. DATE OF REPORT (Yr., Mo., Day) January 1985 — 15. PAGE COUNT 62
16. SUPPLEMENTARY NOTATION N/A	

17. COSATI CODES			18. SUBJECT TERMS (Continue on reverse if necessary and identify by block number)
FIELD	GROUP	SUB. GR.	Avalance Photodiodes, Vapour-Phase-Epitaxy, Passivation.
20	12		

19. ABSTRACT (Continue on reverse if necessary and identify by block number)

Vapour-phase-epitaxial techniques have been used to fabricate InGaAs/InP avalance photodiodes having a "SAM" configuration. The APD's are mesa-etched and are unpassivated. Stable operation up to gains of about 10 has been demonstrated. Noise of all units tested has been somewhat high due to a high value of K_{eff} (~0.6), and due to high bulk dark currents. Attempts to develop a satisfactory passivation for the mesa-etched devices have been largely unsuccessful.

almost 0.6,

Keywords incomplete!

20. DISTRIBUTION/AVAILABILITY OF ABSTRACT UNCLASSIFIED/UNLIMITED ☒ SAME AS RPT. ☐ DTIC USERS ☐	21. ABSTRACT SECURITY CLASSIFICATION UNCLASSIFIED
22a. NAME OF RESPONSIBLE INDIVIDUAL Joseph F. Lorenzo	22b. TELEPHONE NUMBER (Include Area Code) (617) 861-5890 — 22c. OFFICE SYMBOL RADC (ESO)

DEVELOPMENT OF PHOTODETECTORS
FINAL REPORT

1. INTRODUCTION

This is the fourth and final report on this contract. The material presented here includes a summary of all previous effort, as well as work carried out during the final quarter of the program, and during the time extensions which were granted in order to fulfill the requirements of the contract. The period of time covered by the new work reported here is from ~~March~~ JUNE 1, 1983 to ~~May~~ JUNE 30, 1984.

The main effort during this time period has been devoted to fabrication of InGaAs/InP APD's. Thus, most of the new results are related to this work.

2. BACKGROUND

All device fabrication carried out on this program has made use of VPE growth techniques since, within the framework of available knowledge and expertise, this growth method seemed most suitable for the successful fabrication of APD's. Moreover, all previous effort in the growth of InGaAs PIN devices had used the VPE method. Therefore, no work was carried out using LPE techniques. Both single-barrel and double-barrel VPE systems have been used successfully, although in the later stages of this work, particularly for the growth of InGaAs/InP APD's, the single barrel system was used.

In the fabrication of PIN InGaAs/InP photodiodes, carrier concentrations in the undoped InGaAs layer of about $10^{15}/cm^3$ are now routinely obtained, thus enabling the fabrication of photodiodes with low and reproducible capacitance. Moreover, the present growth and fabrication technology yields dark currents for 100μm diameter diodes consistently below 10nA, and frequently below 5nA.

This work has led to a number of standard products of RCA Inc., and data sheets for these products are included in Appendix A, attached to this report. It is to be noted, for example, that the InGaAs photodiodes can be supplied mounted on a ceramic block. This enables customers to incorporate the unit into their own amplifier systems, thus avoiding a number of obvious problems associated with a separately packaged device.

These results, and the effort which has gone into the growth and fabrication technology, have not specifically been a large part of this program, but the effort has been carried out concurrently with the work on this program. This separate work has provided a baseline for the APD work.

3. PASSIVATION

The purpose of this portion of the work was to reduce surface states and dangling bonds that are responsible for carrier recombination and leakage currents. The approach to the problem was two-fold: 1) to attach selected atoms (e.g. hydrogen or nitrogen) to dangling bonds, and 2) to widen the energy gap near the surface, thus creating a potential barrier that would repel both electrons and holes away from the surface. The basis for the work was the successful passivation of silicon by attaching atomic hydrogen to the silicon dangling bonds at the surface. [1]

Details of this part of the work have been discussed in the quarterly reports submitted on this program, and are not reproduced here. In summary, while some evidence of passivation was indicated from photoluminescence measurements on treated surfaces, the effort was only partially successful. InP wafers held at temperatures of about 200°C and above showed evidence of decomposition when exposed to gases (hydrogen, nitrogen or ammonia) which had been atomized by an r.f. glow discharge. At lower temperatures, (150°C), while no decomposition was observed, dark currents of diodes so treated were found to increase substantially.

Analysis of the experimental results has suggested that the limitation in the treatment process may have been due to the presence of trace quantities of oxygen and/or water vapour in the gas sources used for the r.f. glow discharge. The success of Lagowski et al [2] in passivating deep levels in GaAs using atomic hydrogen suggests that further work in this area is warranted, but that oxygen must be eliminated from the glow discharge.

4. InGaAs/InP APD's

4.1 Structure

Initial effort in the fabrication of III-V APD's was concentrated on homojunction InP devices grown on both p-type and n-type substrates. These results have been described in a previous quarterly report. In most devices there was little evidence of gain, suggesting that surface breakdown was occurring long before the bias voltage reached a value where significant internal multiplication occurred. No well defined reasons have been determined for the failure of this earlier work. However, more recent effort with both InP and InGaAs 'SAM' APD's has been considerably more successful. N-type substrate material has been used for all recent work, and the improved results are thought to be due to generally improved growth and device fabrication techniques.

The structure used in these experiments is shown in figure 1a. The finished device is a simple mesa configuration. Contacts to the upper and lower surfaces are made using conventional and previously described techniques. The structure has a number of advantages over other possible devices:

1) Light entry is from the top surface (p^+), similar to the standard line of PIN diodes, so that existing mounting and handling techniques can be used;

2) Light entry from the top avoids the two-fold problem of 2-sided processing (which would be necessary for light entry from the substrate side), and more difficult mounting techniques;

3) Light entry from the top avoids the problem of free-carrier absorption in the substrate which, in some circumstances, results in loss of quantum efficiency;

4) For this structure, long wavelength radiation (e.g. 1.3μm) incident on the top surface is absorbed in that portion of the InGaAs region adjacent to the heterojunction. This is the portion of the InGaAs region which is first to be depleted when the bias voltage exceeds that necessary just to deplete the n-InP region. Thus high quantum efficiency is achieved as soon as a sufficient depth of the InGaAs region is depleted (about 2μm or so), and the InGaAs layer itself does not form a dead layer, (as would be the case for illumination from the substrate side) and therefore the total thickness of the InGaAs layer is not a critical parameter.

There is, however, one important disadvantage to this structure: The use of n-type substrates tends to result in increased fields at the junction on the surface of the etched mesa, which is likely to cause surface breakdown prior to bulk breakdown. For devices fabricated on p-type substrates the conditions tend to favour lower surface fields, and therefore better probability of a true bulk breakdown. (However, as noted above, this did not seem to be the case for results reported earlier in this program).

No matter what the configuration of the APD structure, it seems likely that some technique for surface field reduction will have to be utilized if reliable and stable devices are to be achieved. One possible approach to this problem has been discussed in the 2nd quarterly report. A planar version of the basic diode structure used here has been described by Shirai et al [3] in which a diffused guard-ring was used to avoid edge breakdown. Other approaches may also be possible, and will be the subject of future study.

The basic operation and limitations of the 'SAM' APD structure have been described in considerable detail in the literature, and are therefore presented only briefly here. Avalanche multiplication in InP is found to occur for fields in the range of about 4.5 to 6 x 10^5 volts/cm, depending somewhat on the doping concentration in the InP. For an abrupt junction, the field is related to the doping concentration and depletion layer width by the following:

$$E(x) = \frac{q}{\varepsilon} N(w-x)$$

where: N is the doping concentration in the depleted region,
q is the electronic charge,
ε is the dielectric constant
w is the width depleted by the applied voltage, and x is the distance from the junction.

The maximum field, E_m occurs for x=0, and is given by

$$E_m = \frac{q}{\varepsilon} Nw$$

Thus, for example, if E_m is 5×10^5V/cm (for avalanche), then the product Nw is approximately equal to 3.3×10^{12}/cms. In this case, for a doping concentration of $1 \times 10^{16}/cm^3$, the depletion width at avalanche would be about 3.3μm.

In the 'SAM' APD structure of figure 1a, the thickness and doping concentration of the InP region must be chosen so that depletion into the absorbing InGaAs region occurs before avalanche, but also that the field in the InGaAs region does not exceed about 1.5×10^5 V/cm - the approximate threshold for tunnelling.

The field in the device is somewhat as shown in figure 1b. For the parameters shown, the maximum field is given by

$$E_m = \frac{q}{\varepsilon} [N_{d1}w_1 + N_{d2}w_2]$$

and

$$E_1 = \frac{q}{\varepsilon} N_{d2}w_2$$

Thus, for successful operation of the device, the electric field E_1 must satisfy the following:

$$0 < E_1 < 1.5 \times 10^5 V/cm$$

It is clear that a range of thicknesses and doping concentrations for the InP region is possible for successful fabrication, and depending somewhat on the actual breakdown field, E_m, the product $N_{d1}w_1$ may lie in the approximate range 2.0 to $3.5 \times 10^{12}/cm^2$. It is equally clear, however, that the limits of these parameters are relatively narrow, given the limitations of doping control, layer thickness uniformity and reproducibility of the VPE process. Nevertheless, a number of 'SAM' APD wafers have been fabricated which have yielded diodes having gains of about 10 or greater, and good response at 1.3μm. These results are described below in some detail.

4.2 Experimental Results

The diode pattern used is shown in figure 2. Because slight undercutting of the pattern occurs during the etching process, the actual mesa is found to be slightly smaller than shown. Measurement of actual devices has given an area typically about 1.26×10^{-4} cm^2.

The first results shown are for an APD in which reach-through to the InGaAs region did not occur. Thus, the results obtained are for an InP APD. Measurements of response were made at a wavelength of 900nm, since there was no long-wavelength response, and quantum efficiency decreased dramatically at shorter wavelengths due to absorption in the capping p^+InP layer.

Figure 3 shows the response as a function of bias voltage. In order to determine the gain, the unity gain response has been assumed to increase at higher bias voltages with the same slope as at lower voltages. The unity gain reference line is indicated in the figure. The gain, therefore, can be easily calculated, and is shown in figure 4. It is to be noted that the gain observed is electron gain, since the absorption is all on the p-side of the junction. The hole gain M_h is related to the electron gain M_e by

$$M_e - 1 = k\ (M_h - 1)$$

where, for a peak field of the order of 5×10^5 V/cm in this device, k should be about 0.62 [4]. The dark current is also plotted in figure 4. The dark current increase at high voltages is almost certainly due to the gain and corresponds to an unmultiplied bulk dark current in the device of about .2nA.

The capacitance as a function of bias voltage is shown in figure 5. The slope of less than -.5 is an indication of the junction grading effect due to the diffusion of the zinc from the p^+ InP region to form the junction.

In figure 6, the electron gain of a 'reach-through' InGaAs APD is shown. Since the device has no long wavelength response at low bias voltages, the gain is obtained, as for device #1, above, by measuring at 900nm. The hole gain, calculated from the electron gain using k=0.62, is shown as a dashed curve.

Figure 7 shows the long-wavelength (1300nm) response of the diode. The response is seen to rise rapidly as the depletion layer nears the InP/InGaAs interface, and reaches through into the InGaAs region. The dashed curve shows the calculated unity gain response, which was obtained by dividing by the hole gain from figure 6. For comparison, the response of the reference diode is shown, which is approximately equal to the high voltage unity gain response of the APD. This confirms that the device is well behaved, has high quantum efficiency, and that the assumed k factor is about correct.

The capacitance of this diode is plotted as a function of bias voltage in figure 8. As expected, the capacitance drops precipitously after reach-through, thus defining the reach-through voltage as about 40 volts.

An excessive noise problem has been observed in many diodes, at bias voltages corresponding approximately to the reach-through point. This is shown for another diode, the results of which are plotted in figure 9. In this particular device, the doping concentration and/or thickness of the InP layer was too low, so that the gain after reach-through was found to be only slightly above 1 in the voltage range measured. Nevertheless, the noise of the diode, as shown in the figure, rises to a very high value at about the reach-through voltage, decreasing somewhat at higher voltages.

There is at the present time no explanation for this problem, but it can be assumed that some irregularity in the device structure exists at the hetero-interface.

The results of one further device, from a wafer which showed a much reduced anomalous noise at the reach-through voltage, are shown in Figures 10-14. Figure 10 shows the responsivity and figure 12 shows the estimated hole and electron gains. Fig. 12 shows the dark current and the estimated primary dark current after dividing by the hole gain. Note that unmultiplied dark current, which should be proportional to $w + L_d$, where w is the width of the depletion layer in the InGaAs and L_d the diffusion length, behaves roughly as expected.

Figure 13 shows the calculated excess noise factor as a function of gain and fig. 14 shows the measured and calculated noise. Note that at high gains the calculated noise agrees reasonably well with the measure noise, but that there is still some anomalously large noise at low gains.

4.3 Discussion

There are a number of outstanding problems which must be resolved before a useful device is achieved. These problems will be the subject of future work. In general, gains have been quite low. This is undoubtedly due - at least in part - to high fields at the junction periphery of the device. It will be necessary, therefore, to devise a workable technique for surface field reduction, as discussed earlier in this report.

The noise problem which occurs near the reach-through voltages would severely limit the usefulness of most devices fabricated so far. In addition, the noise of the diodes measured - even the device of figure 10 - are excessively high for the relatively low gains achieved. Much of the excess noise, may arise from high fields, and therefore high localized gains at the etched surface of the mesa. This again indicates the necessity of reducing the peripheral field. At the same time, the active multiplying area could probably be reduced substantially for most fibre-optic applications.

The measured dark current is about an order of magnitude higher than one would like to see in a useful device. Some of this can be reduced by making the device smaller, but more attention will probably have to be paid to interface states, etc. from which the dark current may be coming.

It is also noted that none of the devices fabricated so far has had an intermediate or graded bandgap layer between the n-InP and the undoped InGaAs regions. This layer would be necessary to avoid the slow response characteristic which has been found to be associated with the valence-band discontinuity at the hetero-interface. The development of growth techniques to insert such a layer will be the subject of future work.

4.4 Deliverable InGaAs/InP APD's

Five APD's have been mounted, evaluated, and made available for delivery as a requirement of this program. The diodes have been selected from water B-19, which is the same lot from which the diode of figure 10 was obtained. The measured results for the 5 diodes are attached to this report as Appendix B.

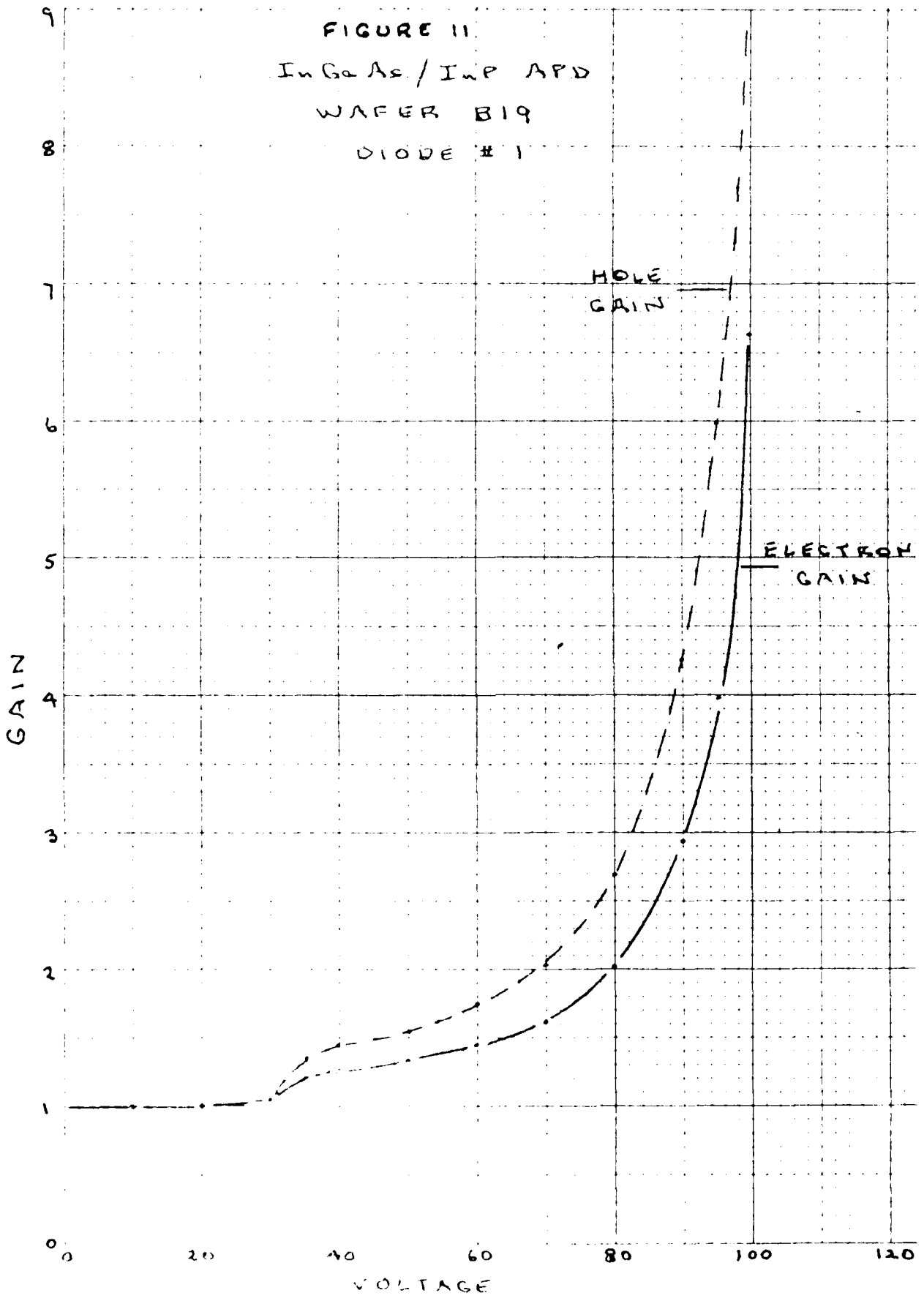
FIGURE 11
InGaAs / InP APD
WAFER B19
DIODE # 1
HOLE GAIN
ELECTRON GAIN
GAIN
VOLTAGE
0
1
2
3
4
5
6
7
8
9
0
20
40
60
80
100
120

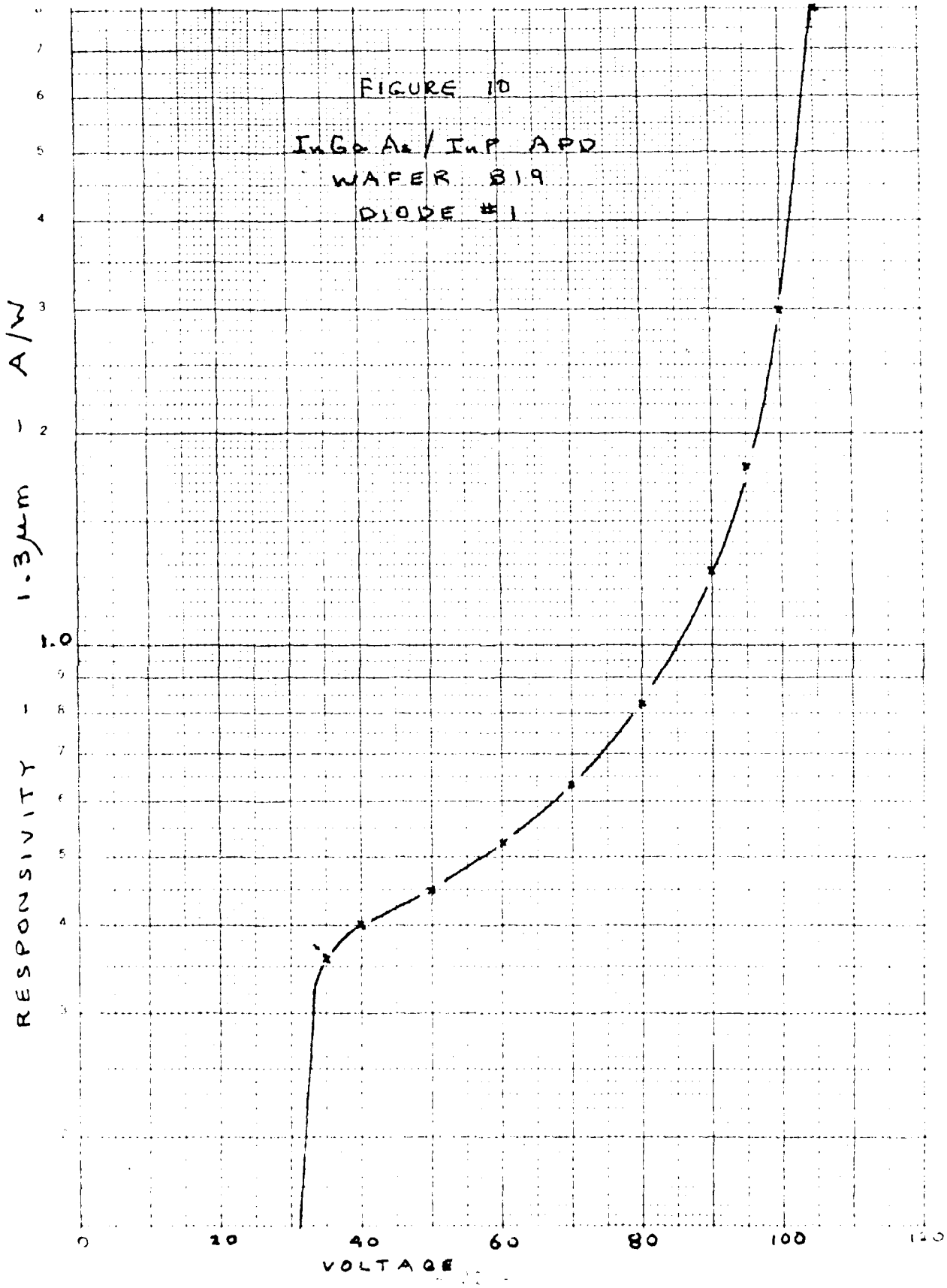
FIGURE 10
InGaAs / InP APD
WAFER B19
DIODE #1
RESPONSIVITY - 1.3μm - A/W
1.0
0
20
40
60
80
100
VOLTAGE

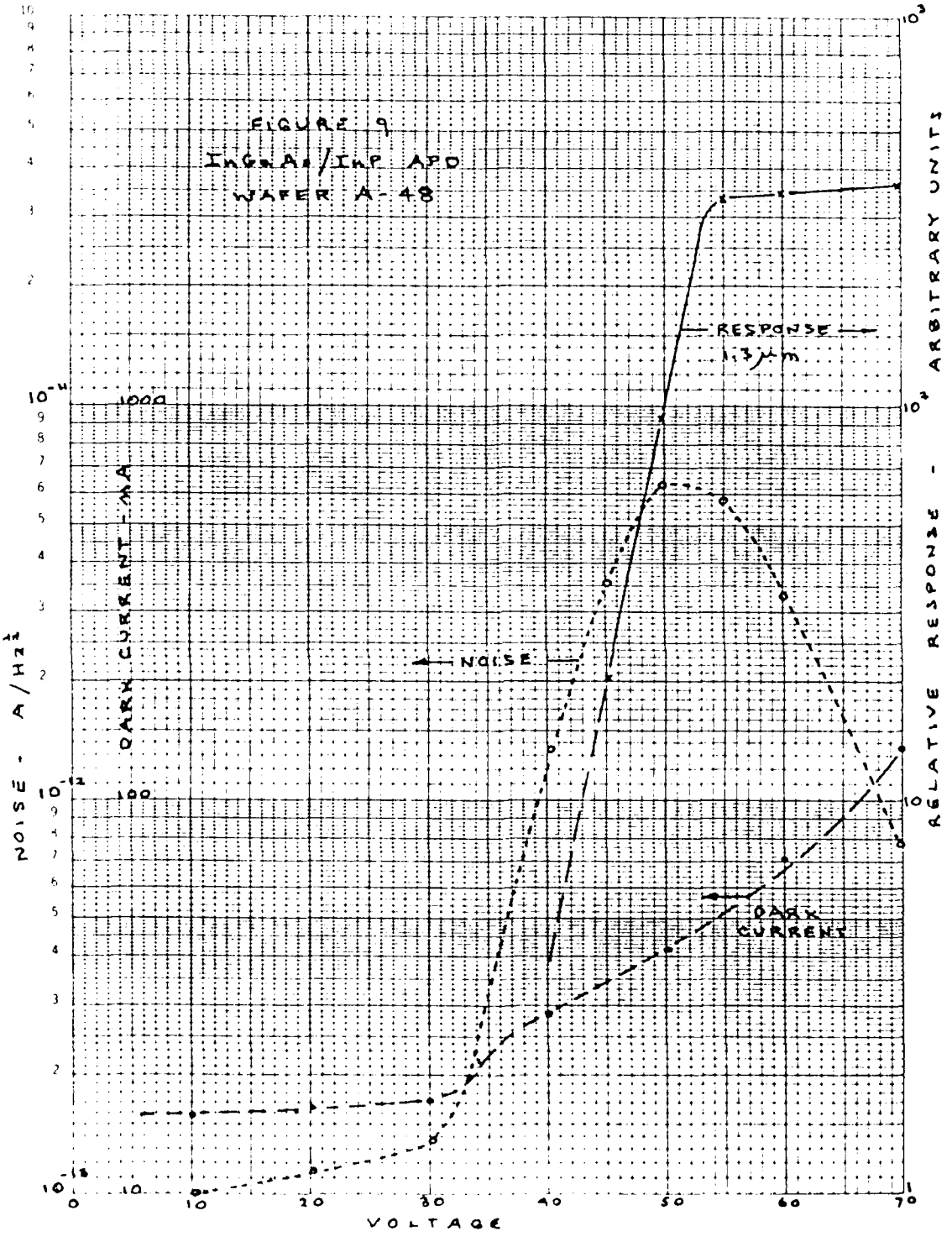
FIGURE 9
InGaAs/InP APD
WAFER A-48
RESPONSE
1.3 μm
NOISE
DARK CURRENT
NOISE - A/Hz^½
DARK CURRENT - mA
RELATIVE RESPONSE - ARBITRARY UNITS
VOLTAGE
0
10
20
30
40
50
60
70

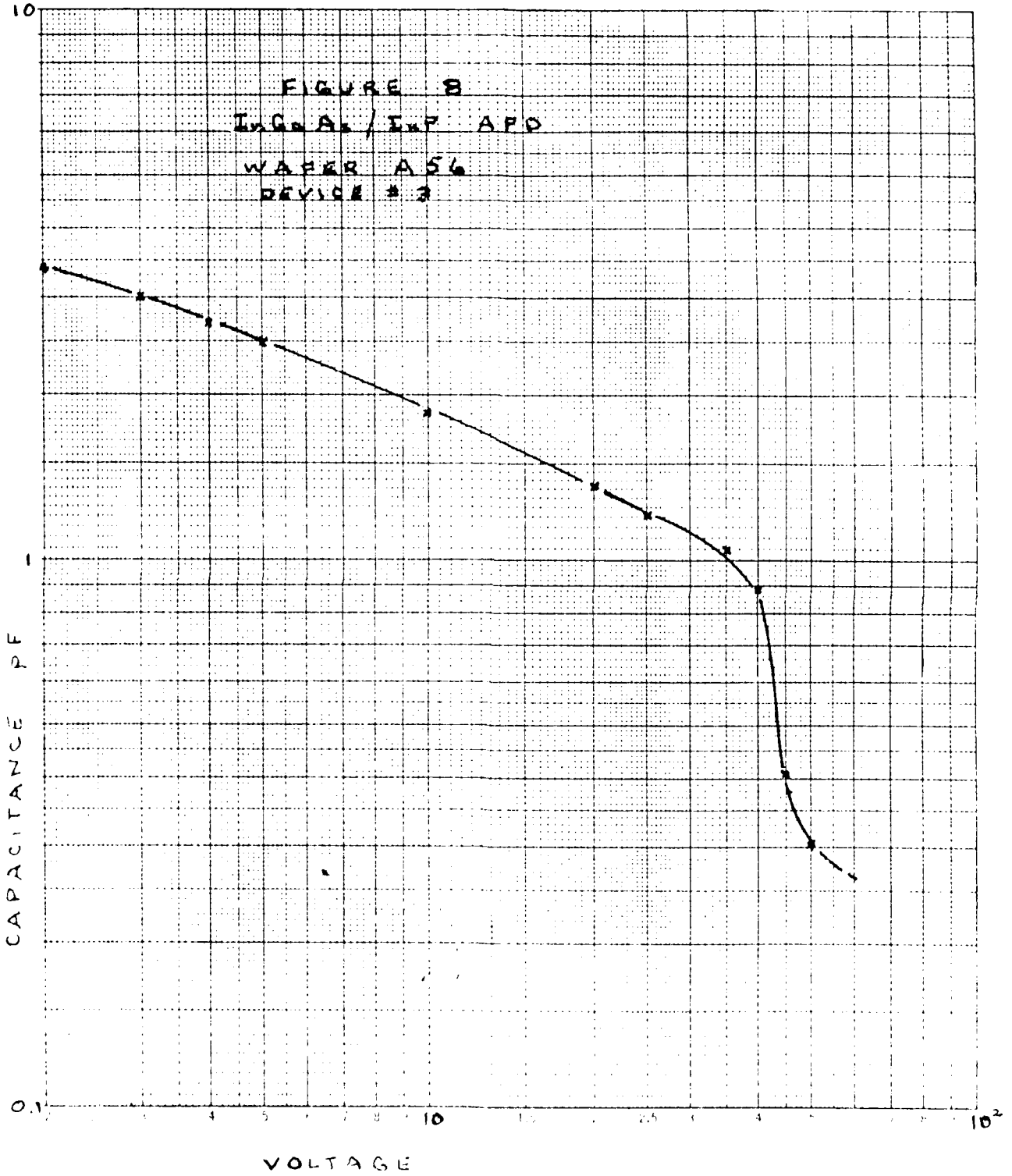
FIGURE 8
InGaAs / InP APD
WAFER A56
DEVICE # 3
10
1
0.1
CAPACITANCE PF
10
10²
VOLTAGE

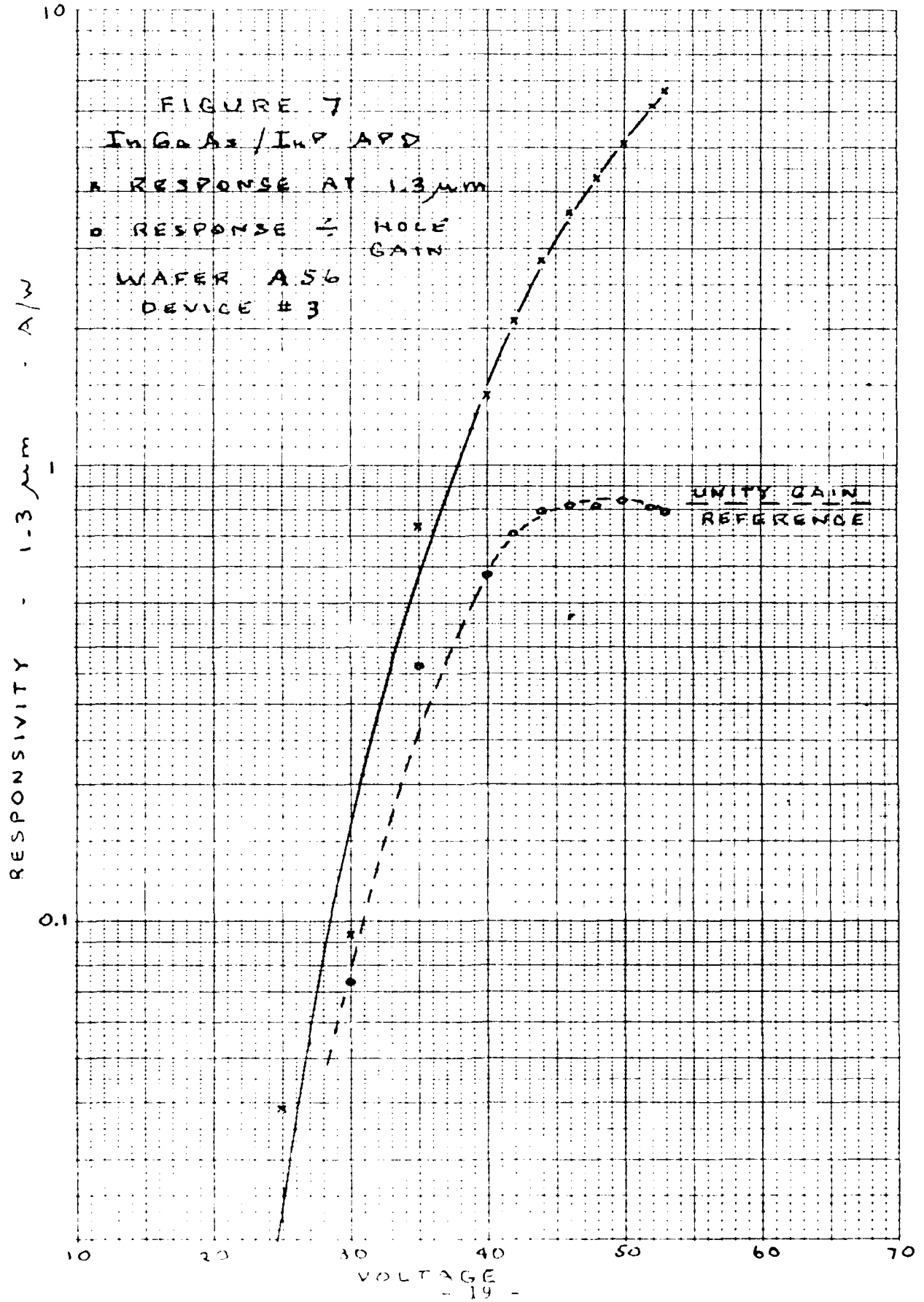
FIGURE 7
InGaAs / InP APD
x RESPONSE AT 1.3 μm
o RESPONSE ÷ HOLE GAIN
WAFER A56
DEVICE #3
UNITY GAIN REFERENCE
RESPONSIVITY - 1.3 μm - A/W
10
1
0.1
10
20
30
40
50
60
70
VOLTAGE

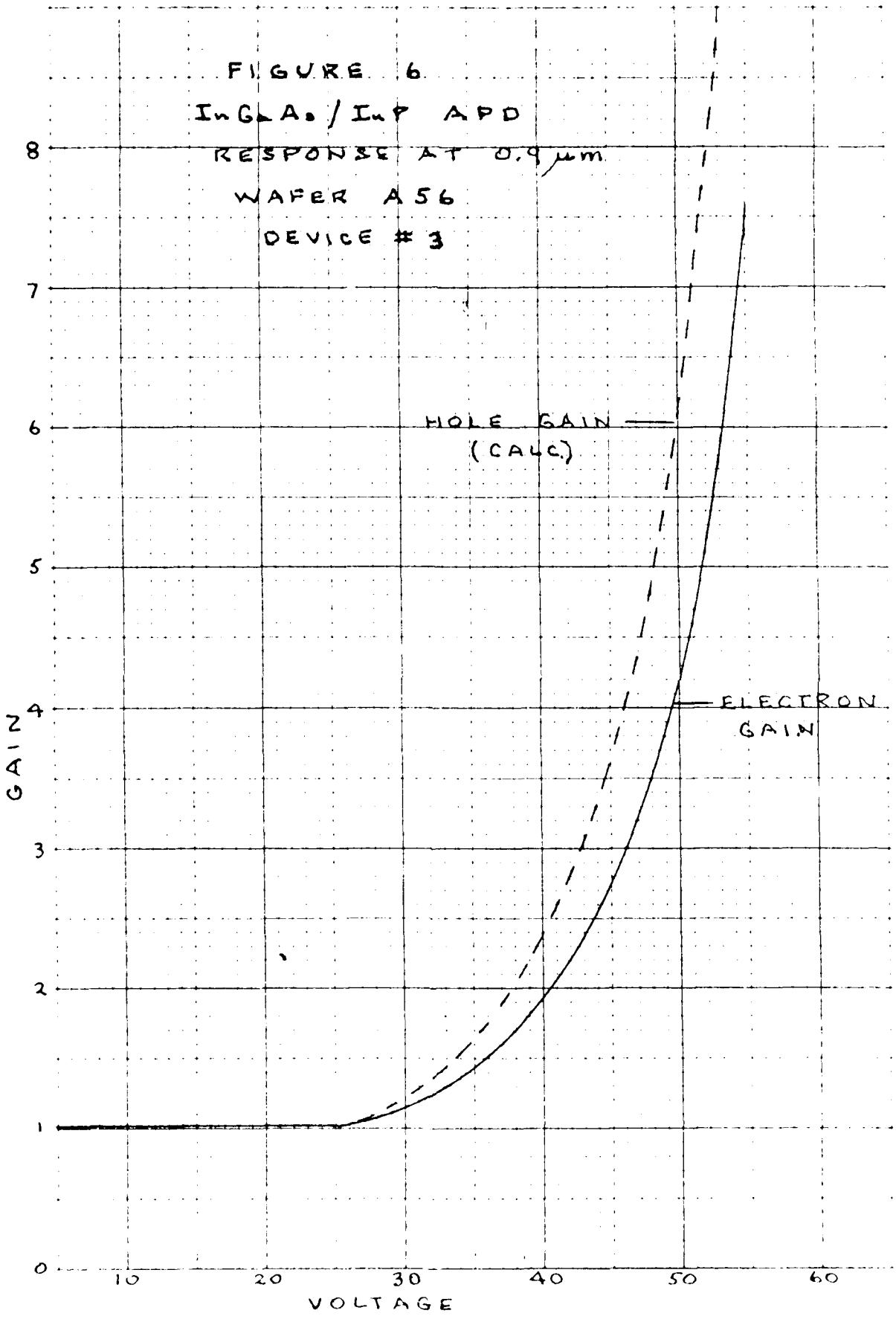
FIGURE 6
InGaAs/InP APD
RESPONSE AT 0.9 μm
WAFER A56
DEVICE #3
HOLE GAIN
(CALC.)
ELECTRON
GAIN
GAIN
VOLTAGE
0
1
2
3
4
5
6
7
8
10
20
30
40
50
60

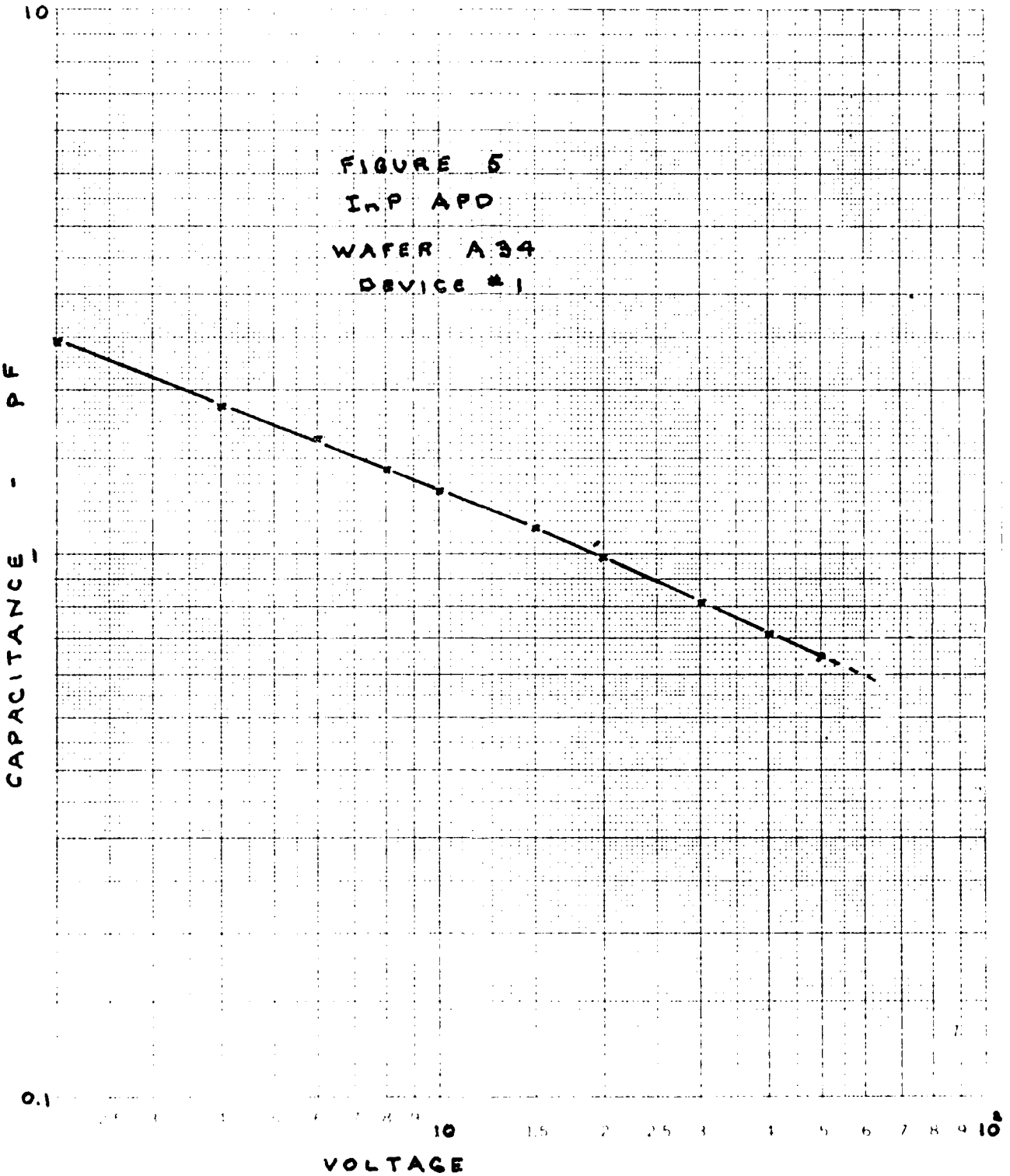
FIGURE 5
InP APD
WAFER A34
DEVICE #1
CAPACITANCE - PF
10
1
0.1
10
1.5
2
2.5
3
4
5
6
7
8
9
10²
VOLTAGE

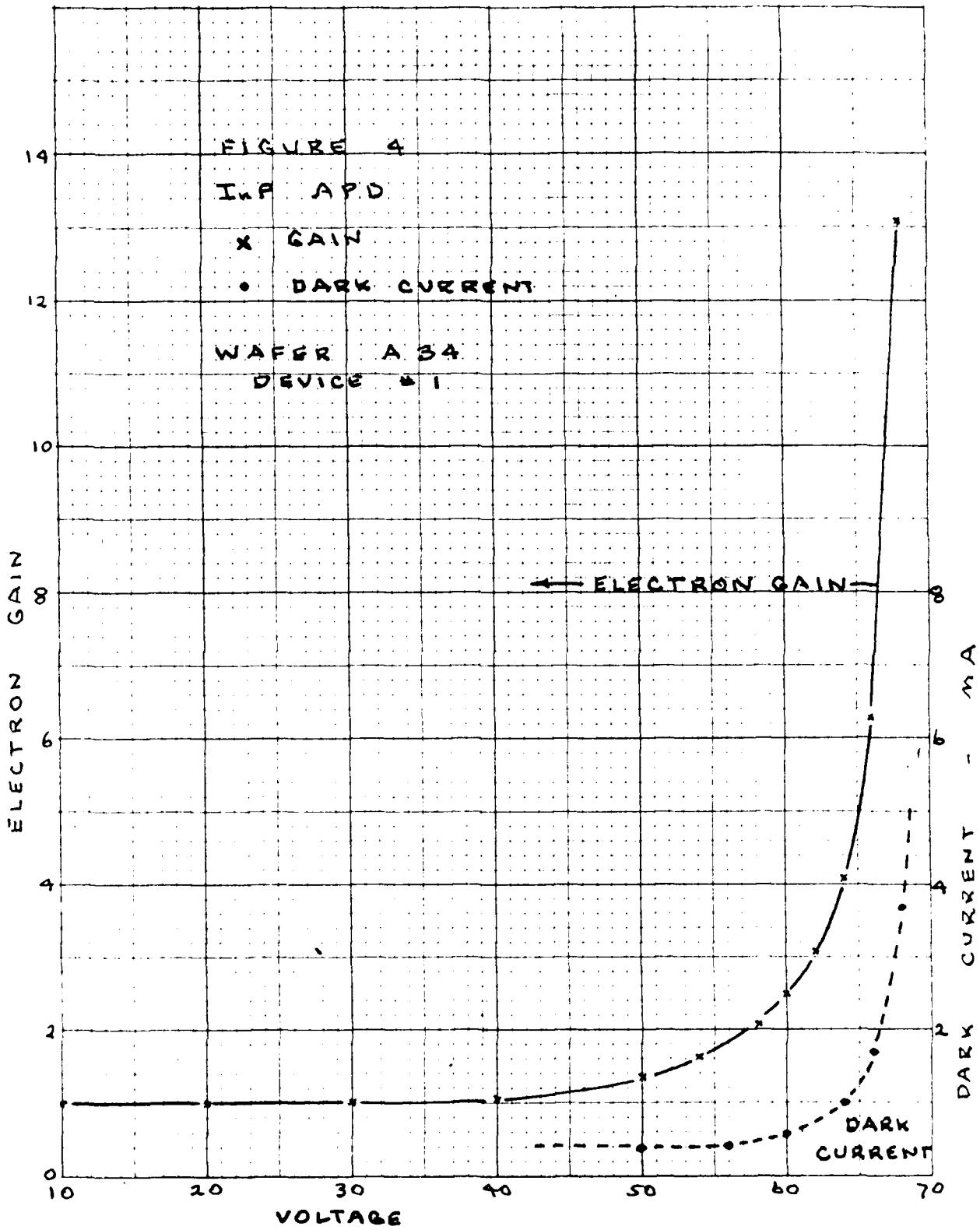
FIGURE 4
InP APD
× GAIN
• DARK CURRENT
WAFER A 34
DEVICE # 1
ELECTRON GAIN
DARK CURRENT
ELECTRON GAIN
DARK CURRENT - mA
VOLTAGE
0
2
4
6
8
10
12
14
10
20
30
40
50
60
70

FIGURE 3

InP APD

WAFER A34

DEVICE # 1

λ = 900 nm

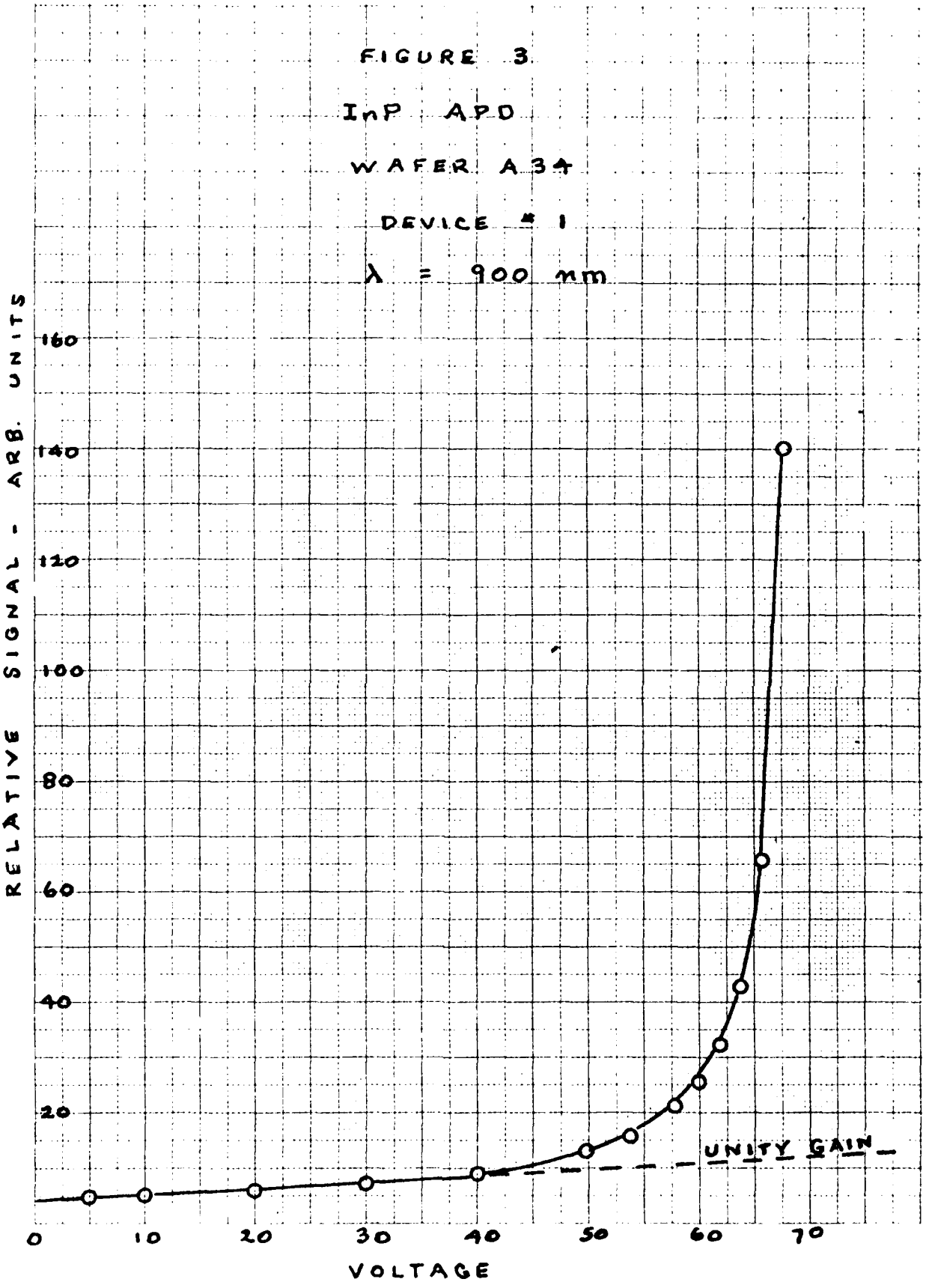

Figure 2

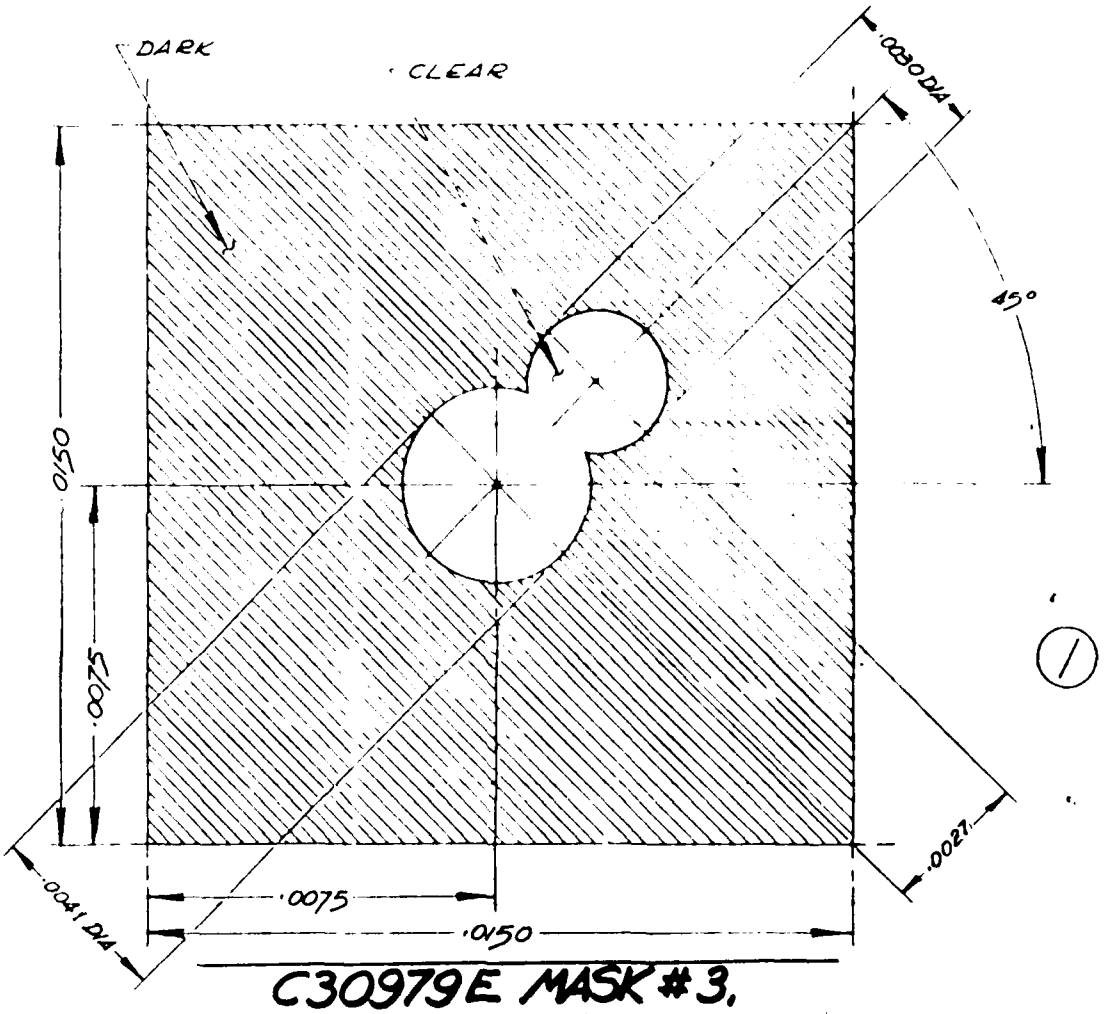

C30979E MASK #3,
MESA ETCH

Figure 1

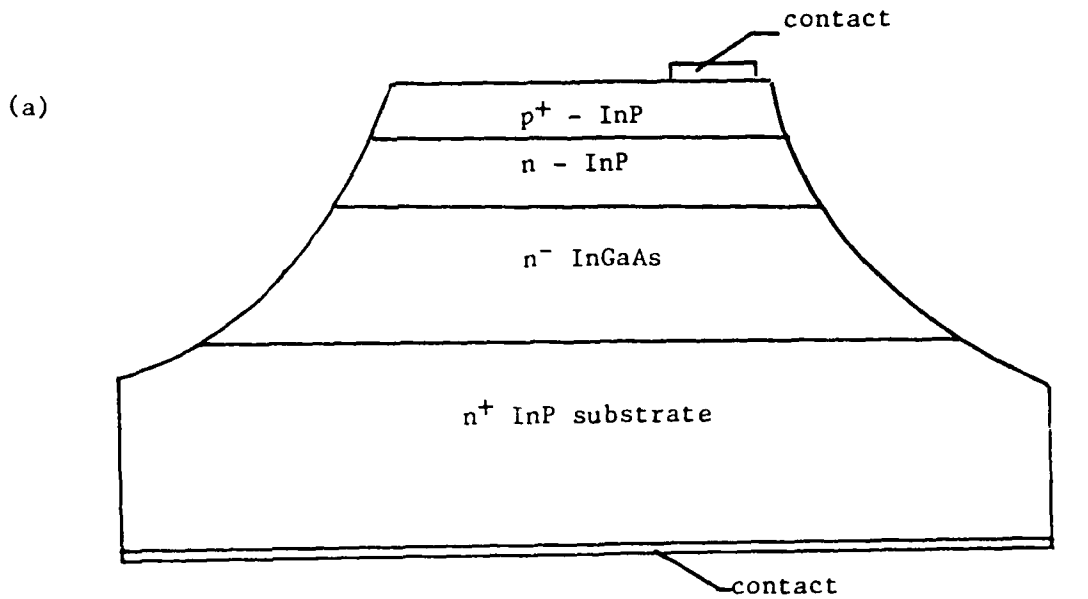
(a)
contact
p+ - InP
n - InP
n- InGaAs
n+ InP substrate
contact

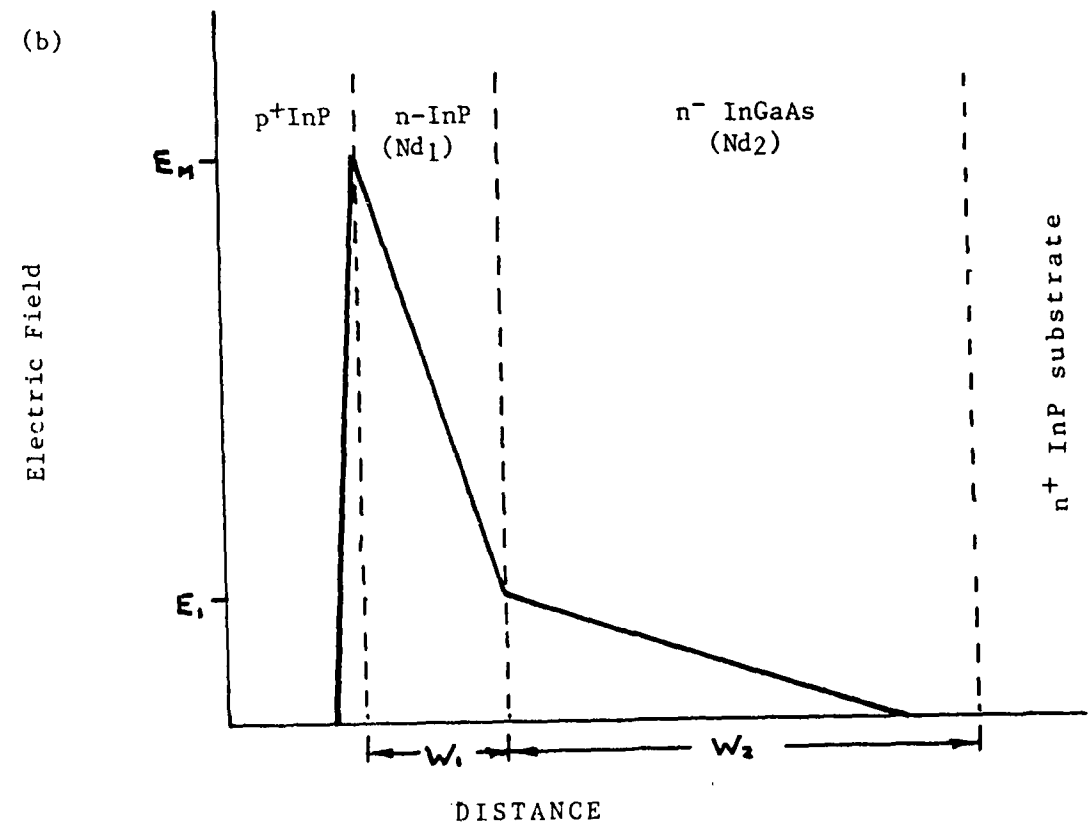
(b)
p+InP
n-InP
(Nd1)
n- InGaAs
(Nd2)
Em
E1
Electric Field
n+ InP substrate
W1
W2
DISTANCE

LIST OF FIGURES

Figure 1a 'SAM' Avalanche Photodiode Structure using N-type Substrate.
Figure 1b Field Profile for 'SAM' APD Structure.

Figure 2 Diode Geometry.

Figure 3 Response of an InP APD at 900nm as a Function of Bias Voltage Showing Assumed Unity Gain Slope.

Figure 4 Electron Gain and Dark Current for Diode of Figure 3.

Figure 5 Capacitance as a Function of Voltage for APD of Figure 3.

Figure 6 Measured Electron Gain and Calculated Hole Gain for an InGaAs/InP APD.

Figure 7 1.3μm Response of Diode of Figure 6. Dashed Curve Shows Response When Divided by Hole Gain.

Figure 8 Capacitance of APD of Figure 6.

Figure 9 InGaAs/InP APD Response, Noise and Dark Current Showing Excess Noise Problem.

Figure 10 1.3μm Response of an InGaAs/InP APD.

Figure 11 Electron and Hole Gain of APD of Figure 10.

Figure 12 Total and Unmultiplied Dark Currents of APD of Figure 10.

Figure 13 Calculated Excess Noise Factor for InGaAs/InP APD's. ($k_{eff} \approx 0.6$).

Figure 14 Measured and Calculated Noise for APD of Figure 10.

There are, therefore, three basic ways of reducing the capacitance of the PIN diode.

1) Decrease the area of the diode.
2) Increase the bias voltage.
3) Decrease the carrier concentration in the (undoped) n^- InGaAs region (i.e. N)

Within the framework of the existing mechanical and electrical design, the area and bias voltage of the detector cannot be changed. Thus, the only parameter remaining for capacitance reduction is the background doping concentration in the n^-InGaAs region. With the continuing wafer fabrication effort described earlier in this report values for the doping concentration in the high 10^{14} and low $10^{15}/cm^3$ range are routinely achieved. Apart from the fabrication effort, optimization of diodes for the PIN-FET receivers has consisted of diode selection for lowest capacitance.

5.2 Deliverable Fibre-Pigtailed PIN-FET Receivers

A requirement of this contract is the delivery of 5 state-of-the-art fibre pigtailed PIN detector devices. For this requirement we have chosen 5 PIN-FET receivers, as described above, the detailed measurements of which are found in Appendix C.

LIST OF REFERENCES

[1] J.I. Pankove, M.A. Lampert, & L. Tarng; Appl. Phys. Lett. 32, 439 (1978).

[2] J. Lagowski, M. Kaminska, J.M. Parsey, H.C. Gatos, & M. Lightensteiger; Appl. Phys. Lett. 41, 1078 [1982].

[3] T. Shirai, S. Yamazaki, H. Kawata, K. Nakajima, & T. Kaneda, I.E.E.E. Trans. Electron Devices, ED-29, 1404, [1982].

[4] See, for example, Ionization Coefficient Data by L.W. Cooke, G.E. Bulman & G.E. Stillman; Appl. Phys. Lett. 40, 589 [1982].

5. PIN-FET RECEIVERS

A development program for a long-wavelength PIN-FET receiver has been carried out in parallel with the work on this contract, but the receiver design effort has not been a part of this program. This work has resulted in a PIN-FET receiver being sold as a standard commercial product of RCA Inc. The receiver uses the best available long wavelength PIN diodes from the detector work. A data sheet for the receiver is included in Appendix A. The product number is C30986E. The necessary fibre-pigtailing and test facilities for these receivers have also been set-up.

Integration of long wavelength PIN diodes with bipolar preamplifiers, as originally proposed, has been replaced, therefore, by the optimization of diodes for the PIN-FET receiver.

5.1 PIN Detector Optimization

The optimization of PIN diodes has consisted mainly of a continuing effort to decrease the capacitance of the diodes, which has a direct effect on the performance of the receiver. In general, the noise of the diode chips is low, and has not contributed significantly to the system noise.

The capacitance of a diode is given by:

$$C = \left[\frac{\varepsilon q N}{2V}\right]^{\frac{1}{2}} A$$

where ε is the dielectric constant
q is the electronic charge
N is the doping concentration
V is the voltage, and
A is the diode area.

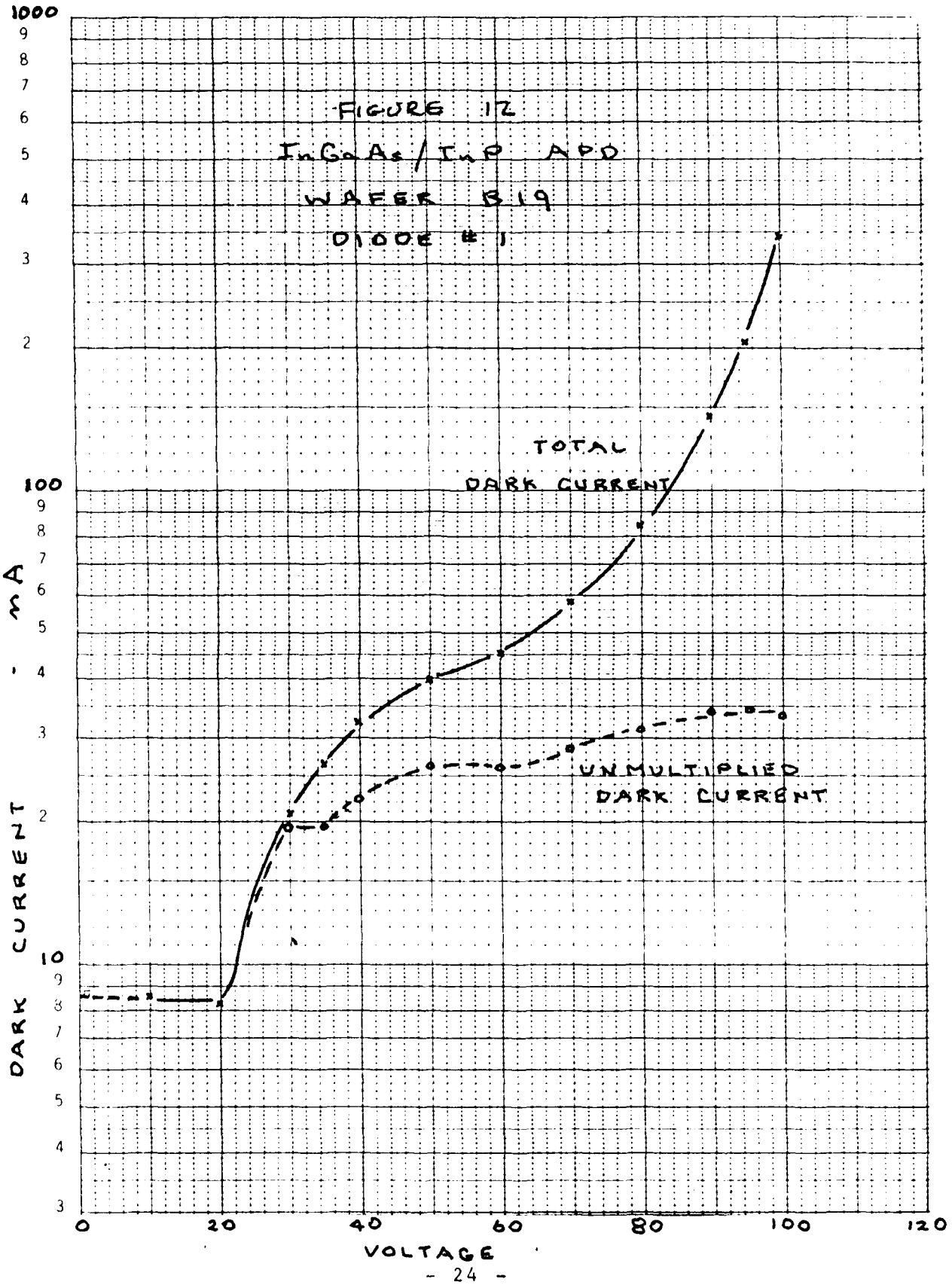
FIGURE 12
InGaAs/InP APD
WAFER B19
DIODE # 1
TOTAL
DARK CURRENT
UNMULTIPLIED
DARK CURRENT
DARK CURRENT - mA
VOLTAGE
1000
100
10
0
20
40
60
80
100
120

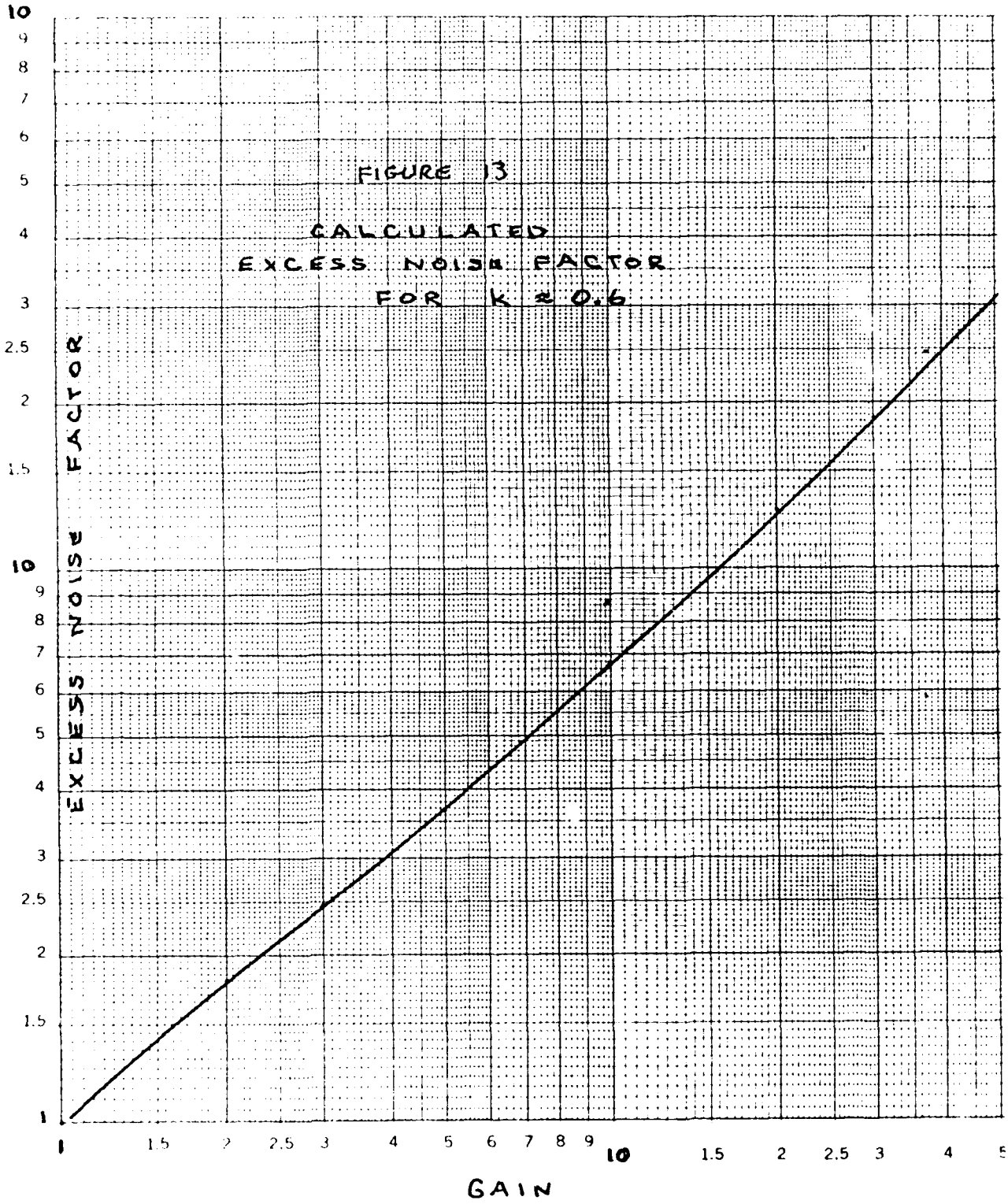

FIGURE 13

CALCULATED

EXCESS NOISE FACTOR

FOR $k \approx 0.6$

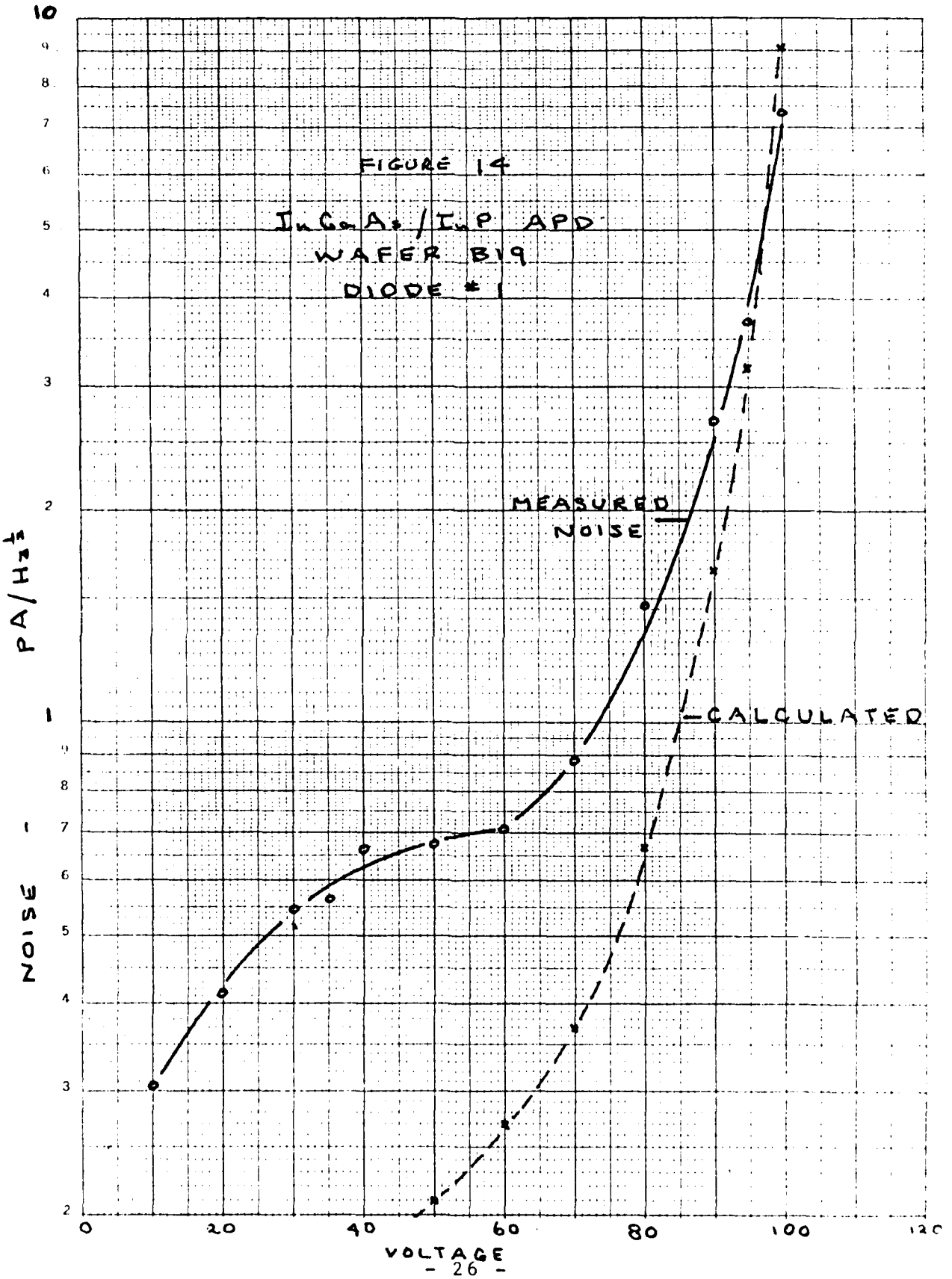
FIGURE 14
InGaAs / InP APD
WAFER B19
DIODE # 1
MEASURED NOISE
CALCULATED
NOISE - PA/Hz^½
VOLTAGE
10
9
8
7
6
5
4
3
2
1
9
8
7
6
5
4
3
2
0
20
40
60
80
100
120

APPENDIX A

DATA SHEETS FOR
CURRENT RCA STANDARD
PRODUCTS

RCA Electro Optics and Devices

Solid State Detectors
Developmental Types

C30979E, C30980E, C30980EL

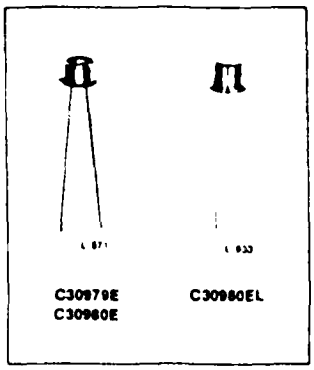

Photodiodes

Indium Gallium Arsenide Photodiodes for Detection of 900 to 1700 nm Radiation

- **High Quantum Efficiency -**
  70% typical at 1300 and 1550 nm
- **Spectral Response Range -**
  900 to 1700 nm
- **Extremely Fast Time Response -**
  Rise time typically less than 1.0 ns
  Fall time typically less than 1.0 ns

RCA Developmental Types C30979E and C30980E are high speed Indium Gallium Arsenide/Indium Phosphide photodiodes. These structures provide high responsivity and very fast response between 900 and 1700 nanometers and are optimized for detection of 1300 nm and 1550 nm sources. They are particularly useful for fiber optic communications at these wavelengths. These devices are supplied in a TO-18 package with a removable cap which permits optimum coupling of the fiber to the active area of the detector. These devices can be supplied sealed behind a flat glass window on request.

The C30980EL is supplied in a hermetically sealed package which incorporates a short light pipe as an integral part of the package. The light pipe is positioned close enough to the detector's active area that most of the radiation exiting from the light pipe falls within the active area of the detector. This hermetically sealed package allows fibers to be epoxied to the end of the light pipe to minimize losses without fear of endangering detector stability.

The C30979E and C30980E are also available mounted on a ceramic block for hybrid work (see Figure 4). In this configuration the type numbers are C30979CER and C30980CER.

Maximum Ratings, Absolute-Maximum Values[1]

Reverse Bias Dark Current	500	μA
Photocurrent at 22° C:		
Average value, continuous operation	0.5	mA
Peak value (For 1 second duration, non-repetitive)	1.0	mA
Forward Current, I_F at 22° C:		
Average value, continuous operation	0.1	mA
Peak value (For 1 second duration, non-repetitive)	0.5	mA
Maximum Total Power Dissipation at 22° C	1	mW
Ambient Temperature —		
Storage, T_{stg}	-60 to +100	°C
Operating, T_A	-46 to +71	°C
Soldering:		
For 5 seconds	200	°C

[1] These are limiting values of operating and environmental conditions. Exceeding these values can cause damage to the device.

For further information or application assistance on these devices, contact your RCA Sales Representative or Photodetector Marketing, RCA, Ste. Anne de Bellevue, Quebec, Canada H9X 3L3 (514) 457-9000

Printed in U.S.A./9-82
C30979E, C30980E, C30980EL
Supersedes C30979E 5-81

Electrical Characteristics	At an ambient temperature (T_A) of 22° C, DC reverse operating voltage V_R = 5 V									Units
	C30979E			C30980E			C30980EL			
	Min.	Typ.	Max.	Min.	Typ.	Max.	Min.	Typ.	Max.	
Recommended Operating Voltage	1	5	10	1	5	10	1	5	10	V
Breakdown Voltage, V_{BR}	30	60	-	30	60	-	30	60	-	V
Responsivity										
At 1300 nm	0.63	0.73	-	0.63	0.73	-	0.50	0.60	-	A/W
At 1550 nm	0.75	0.88	-	0.75	0.88	-	0.60	0.72	-	A/W
Quantum Efficiency										
At 1300 nm	60	70	-	60	70	-	48	58	-	%
At 1550 nm	60	70	-	60	70	-	48	58	-	%
Total Dark Current, I_d	-	15	30	-	150	250	-	150	250	nA
Noise Current, i_n										
f = 10 kHz, Δf = 1.0 Hz	-	0.2	0.4	-	0.3	0.6	-	0.3	0.6	$pA/Hz^{1/2}$
Capacitance, C_d	-	1	2	-	5	10	-	5	10	pF
Rise Time, t_r										
10% to 90% points	-	-	1	-	-	3	-	-	3	ns
Fall Time										
90% to 10% points	-	-	1	-	-	3	-	-	3	ns
Photosensitive Surface										
Shape	Circular			Circular			Not Applicable			-
Useful area	0.008			0.2						mm^2
Useful diameter	100			500						µm

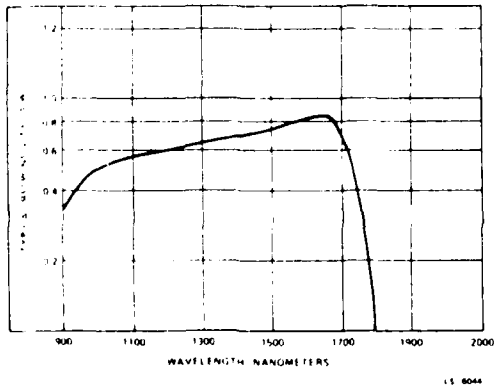

Figure 1 - Typical Spectral Responsivity Characteristic

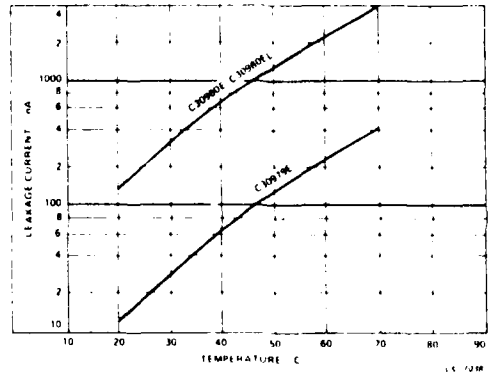

Figure 2 - Typical Leakage Current vs Temperature

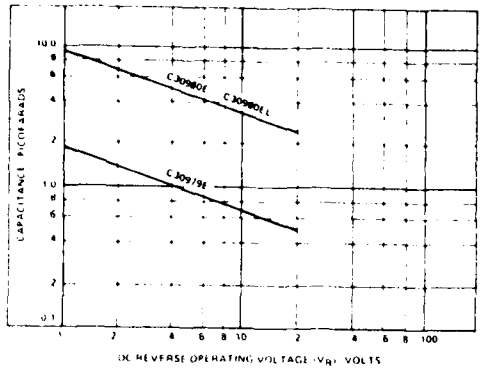

Figure 3 - Typical Photodiode Capacitance vs Operating Voltage

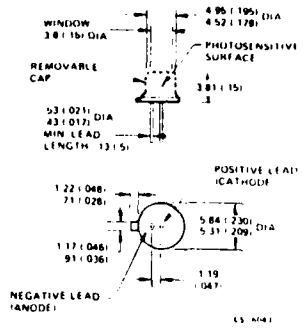

Modified TO-18 Package

Dimensions in millimeters. Dimensions in parentheses are in inches

Figure 5 - Dimensional Outline - C30979E, C30980E

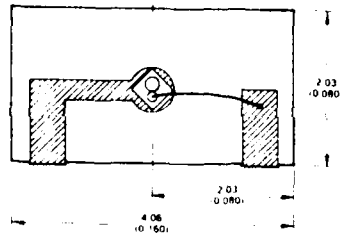

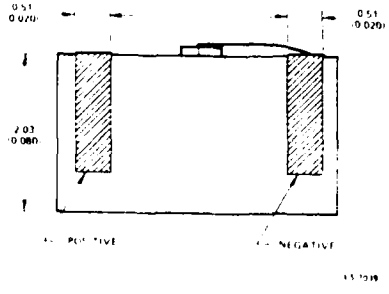

Dimensions in millimeters. Dimensions in parentheses are in inches

Figure 4 - Dimensional Outline - C30979CER, C30980CER

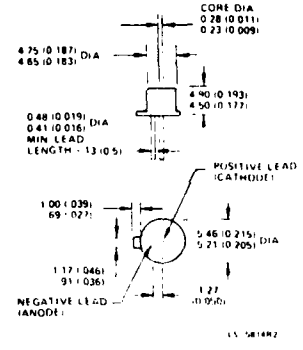

TO-18 Package

Dimensions in millimeters. Dimensions in parentheses are in inches

Figure 6 - Dimensional Outline - C30980EL

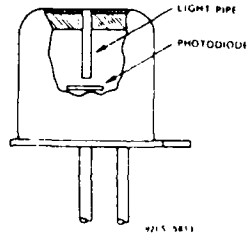

Figure 7 - Cutaway of the RCA C30980EL

RCA Electro Optics and Devices

Solid State Detectors
Developmental Types

C30986E Series

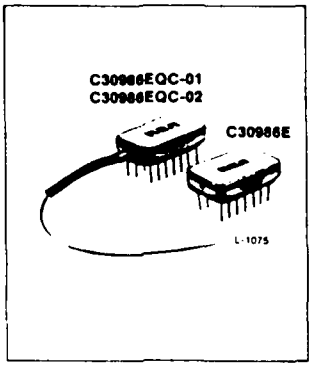

Long Wavelength Photodiode -
Transimpedance Preamplifier Modules
Available with Integral Fiber Optic Pigtail

- **System Bandwidth (3 dB Point) - DC to 250 MHz**
- **Responsivity at T_A = 22° C - $5x10^3$ V/W at 1.3 μm, $6x10^3$ V/W at 1.55 μm**
- **Spectral Response Range - 900 to 1700 nm**
- **Hermetically-Sealed 14-Pin Dual In-Line Packages**
- **Sensitivity (signal-to-noise ratio - 22 dB for B.E.R. = 10^{-9}) - -35 dBm average optical power at 250 MHz**
- **System Noise Equivalent Power (NEP) at T_A = 22° C - 3 pW/$Hz^{1/2}$ at 1.3 μm, 2.5 pW/$Hz^{1/2}$ at 1.55 μm**

RCA Developmental Type C30986E is an Indium Gallium Arsenide (p-i-n) photodiode with a hybrid preamplifier supplied in a 14-pin dual in-line package; a glass window providing optical access to the photodiode is included. RCA Developmental Types C30986EQC-01 and C30986EQC-02 are Indium Gallium Arsenide (p-i-n) photodiodes with hybrid preamplifiers supplied in a 14-pin dual in-line package; this package is supplied with a 50 μm graded index fiber pigtail.

The p-i-n photodiode used in these devices is a high-speed Indium Gallium Arsenide/Indium Phosphide photodiode providing high responsivity between 900 and 1700 nm and is optimized for detection of 1300 and 1550 nm sources.

The preamplifier is a transimpedance type employing a low noise GaAs FET front-end and a cascode feedback circuit. An emitter follower-stage is added to the output to provide improved output coupling efficiency. The system bandwidth for the C30986E Series is typically 250 MHz. Greater sensitivities with correspondingly reduced bandwidths are available.

Absolute-Maximum Ratings, Limiting Values[1]

Photodiode Bias Voltage, V_R		
At T_A = 22° C	-30	V
Preamplifier Voltage		
Positive, $+V_{cc}$	+6.3	V
Negative, $-V_{cc}$	-6.3	V
Incident Radiant Flux, Φ_M (T_A = 22° C)		
Average value	0.6	mW
Peak value (1 sec duration, non-repetitive)	1.2	mW
Ambient Temperature		
Storage, T_{stg}	-50 to +100	C
Operating, T_A	-40 to +70	C

[1] These are limiting values of operating and environmental conditions. Exceeding these values can cause damage to the device.

Mechanical Characteristics

Type	Diode Chip (Dia.)	Fiber Type	Fiber Optic Core Dia.
C30986E	C30979E (100 μm)	-	-
C30986EQC-01	C30979E (100 μm)	Siecor 3008D[2]	50 μm
C30986EQC-02	C30979E (100 μm)	ITT T1271-15[3]	50 μm

[2] A product of Siecor Optical Cables, Inc., Hickory, NC 28601

[3] A product of ITT Electro Optical Products Div., Roanoke, VA 24019

For further information or application assistance on these devices, contact your RCA Sales Representative or Photodetector Marketing, RCA, Ste Anne de Bellevue, Quebec, Canada H9X 3L3 (514) 457-9000

Printed in U.S.A./1-83
C30986E Series

Electrical Characteristics*	C30986E			C30986EQC-01, C30986EQC-02			Units
	Min.	Typ.	Max.	Min.	Typ.	Max.	
Responsivity							
At 1.3 μm	$4x10^3$	$5x10^3$	-	$3x10^3$	$4x10^3$	-	V/W
At 1.55 μm	$5x10^3$	$6x10^3$	-	$4x10^3$	$5x10^3$	-	V/W
Noise Equivalent Power (NEP): 100 kHz $<f<f_c/2$							
At 1.3 μm	-	3.0	5.0	-	3.8	6.8	$pW/Hz^{1/2}$
At 1.55 μm	-	2.5	4.0	-	3.0	5.0	$pW/Hz^{1/2}$
Output Spectral Noise Voltage Density:							
$f = 100$ kHz - f_c $\Delta f = 1.0$ Hz	-	15	20	-	15	20	$nV/Hz^{1/2}$
Output Impedance	-	20	40	-	20	40	Ω
System Bandwidth, f_c (3 dB point)	200	250	-	200	250	-	MHz
Rise Time, t:							
$\lambda = 1.3$ μm and 1.55 μm 10% to 90% points	-	1.5	2	-	1.5	2	ns
Fall Time							
$\lambda = 1.3$ μm and 1.55 μm 90% to 10% points	-	1.5	2	-	1.5	2	ns
Dynamic Range:							
22 dB SNR squarewave	18	20	-	18	20	-	dB
Output Offset Voltage	-0.7	-1.5	-3.0	-0.7	-1.5	-3.0	V
Supply Current:							
+5.0 V	-	25	35	-	25	35	mA
-5.2 V	-	10	15	-	10	15	mA

* At an ambient temperature (T_A) of 22° C, negative photodiode bias of -5.2 VDC, preamplifier operating voltages of +5.0 VDC and -5.2 VDC, and the signal output AC (capacitively) coupled into a 50 ohm termination.

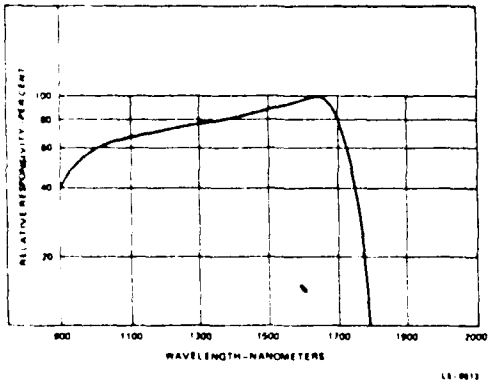

Figure 1 - Typical Spectral Responsivity Characteristic

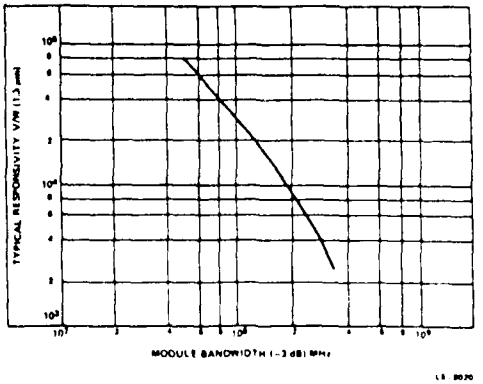

Figure 2 - Projected Bandwidth vs Responsivity (1.3 μm)
(Modules with performance lying on this curve can be made on a custom basis.)

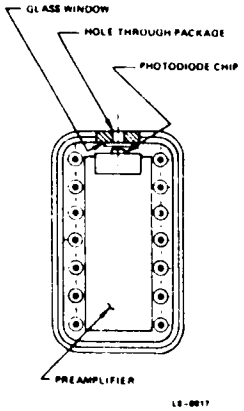

Figure 3 - Package with Cover Removed

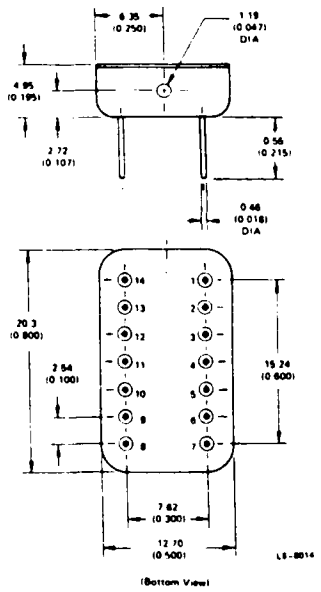

Dimensions in millimeters. Dimensions in parentheses are in inches

Pin Connections

1. Negative Bias for Photodiode
2, 6, 9, 11, 12, 13, 14: No Connection, Do Not Use
3, 5, 8 Ground (Case and Power Supply)
4 $-V_{cc}$ Negative Bias for Amplifier
7 Signal Output
10 $+V_{cc}$ Positive Bias for Amplifier

Figure 4 - Dimensional Outline - C30986E

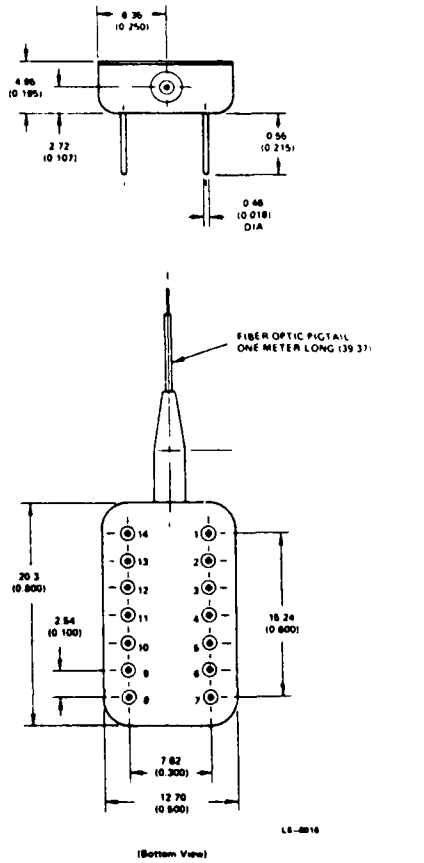

Dimensions in millimeters. Dimensions in parentheses are in inches.

Pin Connections

1: Negative Bias for Photodiode
2, 6, 9, 11, 12, 13, 14: No Connection, Do Not Use
3, 5, 8: Ground (Case and Power Supply)
4: $-V_{cc}$ Negative Bias for Amplifier
7: Signal Output
10: $+V_{cc}$ Positive Bias for Amplifier

Figure 5 - Dimensional Outline - C30986EQC-01, C30986EQC-02

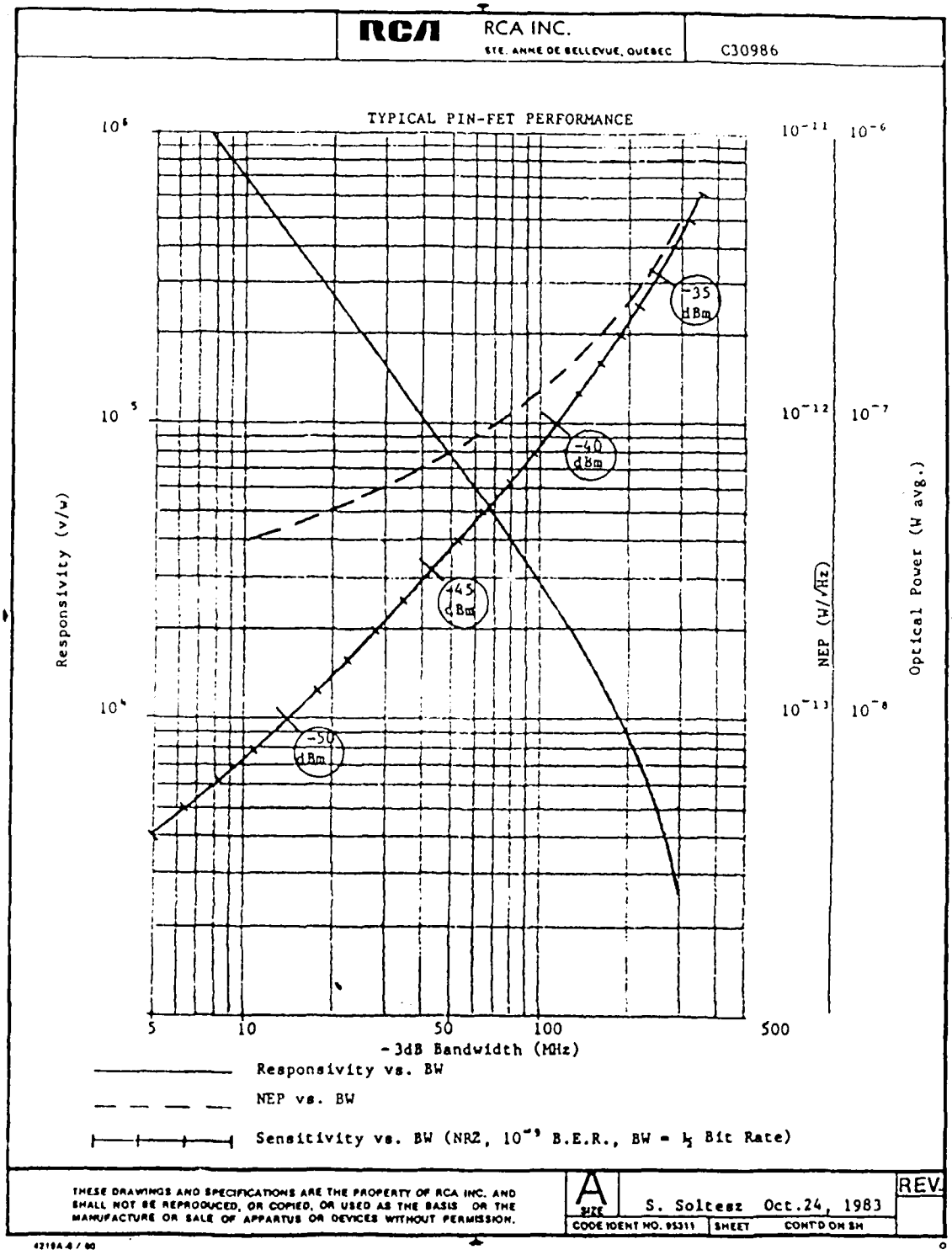

Reprinted with Permission

APPENDIX B

MEASUREMENT DATA FOR
5 INGAAS/INP APD'S
SUPPLIED AS PART OF THE
REQUIREMENTS OF THIS CONTRACT

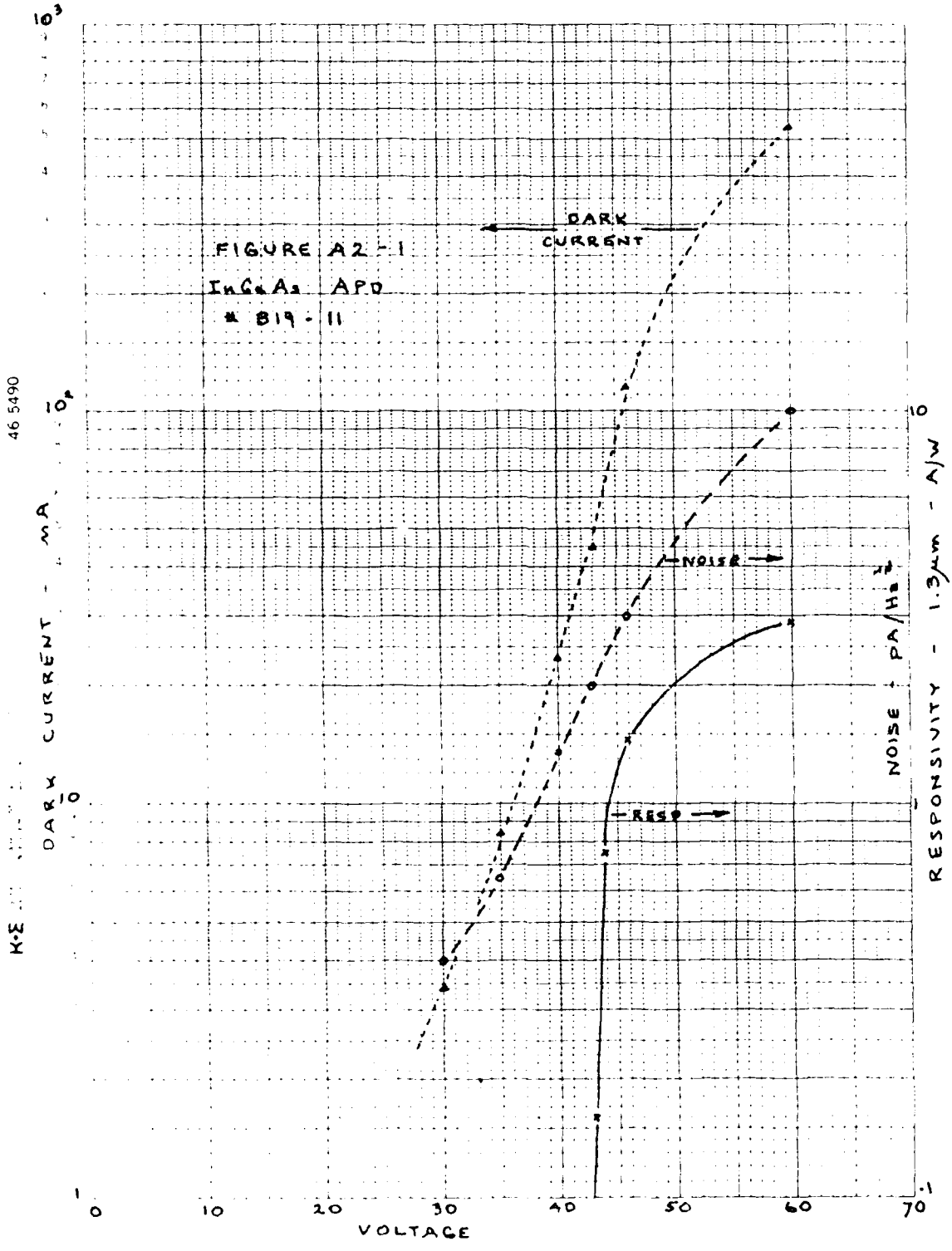
FIGURE A2-1
InGaAs APD
B19-11
DARK CURRENT
NOISE
RESP
DARK CURRENT - mA
NOISE - pA/Hz^½
RESPONSIVITY - 1.3μm - A/W
VOLTAGE
10³
10²
10
1
10
1
·1
0
10
20
30
40
50
60
70

46 5490

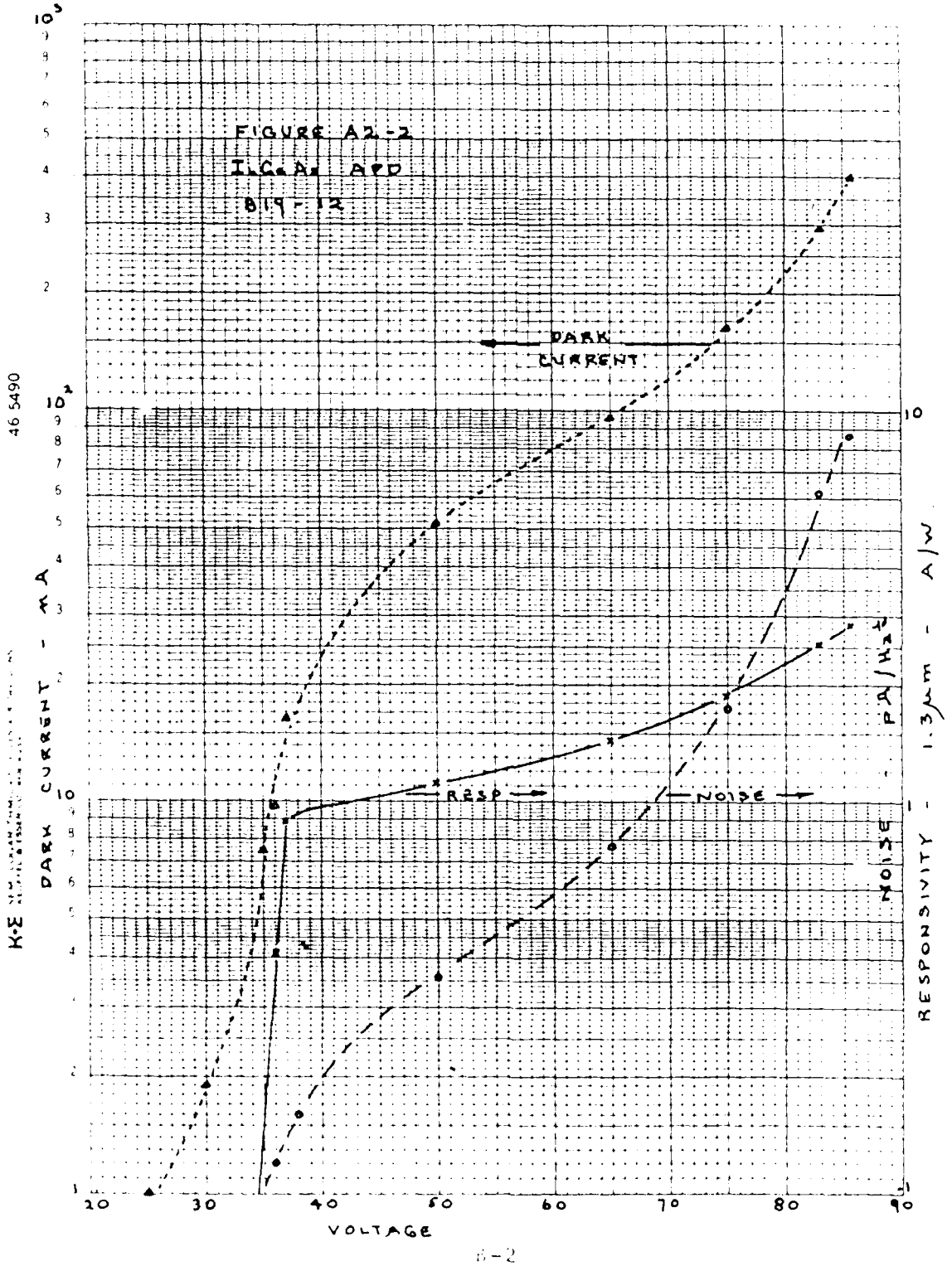
FIGURE A2-2
InGaAs APD
819-12
DARK CURRENT
RESP
NOISE
DARK CURRENT - mA
RESPONSIVITY - 1.3μm - A/W
NOISE - pA/Hz½
VOLTAGE
20
30
40
50
60
70
80
90
46 5490

Electrical Characteristics C30986-70QC-01

	Min.	Typ.	Max.	Units
Detector Responsivity (coupled) @1.3μm	.57	.66	-	A/W
@1.55μm	.68	.79	-	A/W
Responsivity @1.3μm	3.1×10^4	4.2×10^4	-	V/W
@1.55μm	3.6×10^4	5.0×10^4	-	V/W
Noise Equivalent Power (NEP):				
(100KHz f fo/2) @1.3μm	-	1.4	2.6	$pW/\sqrt{Hz}$
@1.55μm	-	1.2	2.2	$pW/\sqrt{Hz}$
Output Spectral Noise Voltage Density				
(f=100KHz-fo, Δf=1.0Hz)	-	60	80	$nV/\sqrt{Hz}$
Sensitivity (Pavg.@10^{-9}B.E.R.)@1.3μm	-42	-43	-	dBm
@1.55μm	-43	-44	-	dBm
Output Impedance		20	40	Ω
System Bandwidth, fo (3dB point)	55	70	-	MHz
Rise Time (10% to 90%)	-	5	6.4	ns
Fall Time (90% to 10%)	-	5	6.4	ns
Dynamic Range (optical)	18	20	-	dB
Output Offset Voltage	-0.7	-1.5	-3.0	V
Supply Current, +5.2V.	-	25	35	mA
-5.2V.	-	10	15	mA
Detector Leakage Current, -5.2V.	-	10	30	nA
Detector Capacitance, -5.2V.	-	0.5	-	pF
Transimpedance Resistor	-	100	-	kΩ

At an ambient temperature (T_A) of 22°C, negative photodiode bias of -5.2VDC, preamplifier operating voltages of +5.2VDC and -5.2VDC, and the signal output AC (capacitively) coupled.

S/N: 0101 TEST SUPERVISOR: L Cutolo DATE: Jan 28/89

CD: _____ Q.C.: _____ DATE: _____

Measured Values

Responsivity @1.3μm	4.2×10^4	V/W into 50Ω
" "	7.0×10^4	V/W into 1000Ω
Detector Leakage Current @5.2V	12	mA
Supply Current, +5.2V	24	mA
" " -5.2V	8.5	nA
Output Offset Voltage	-2.20	V
Output Impedance	34	Ω
System Bandwidth, fo (3dB point)	7	MHz into 50Ω
System Bandwidth "	70	MHz into 1000Ω
Output Spectral Noise Voltage Density (AVG)	43	$nv/\sqrt{Hz}$ into 50Ω
" " " " " (Peak)	65	" " "

C30986 Series

S/N: 0101 TEST SUPERVISOR: JC DATE: June 28/89

CD: _____ Q.C.: _____ DATE: _____

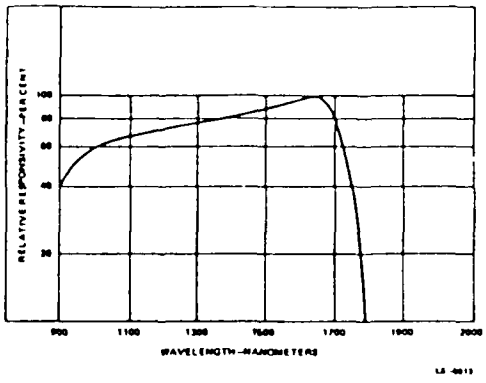

- Typical Spectral Responsivity Characteristic

- Dimensional Outline -

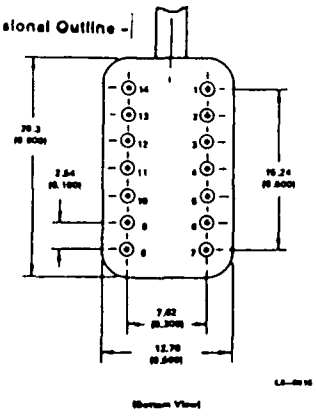

Dimensions in millimeters. Dimensions in parentheses are in inches.

Pin Connections

1: Negative Bias for Photodiode
2, 6, 9, 11, 12, 13, 14: No Connection, Do Not Use
3, 5, 8: Ground (Case and Power Supply)
4: $-V_{oa}$ Negative Bias for Amplifier
7: Signal Output
10: $+V_{oa}$ Positive Bias for Amplifier

2dB/div

20nV/Hz$^{1/2}$ /div

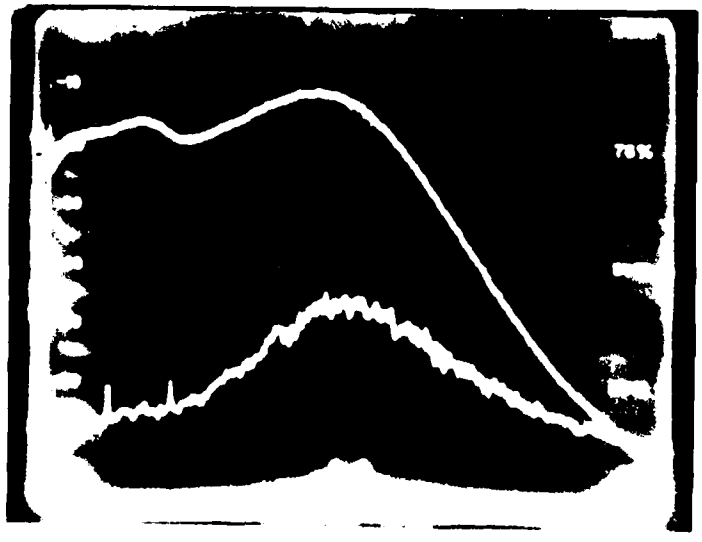

o/p Load: 50 ohms

Electrical Characteristics C30986-70QC-01

	Min.	Typ.	Max.	Units
Detector Responsivity (coupled) @1.3μm	.57	.66	-	A/W
@1.55μm	.68	.79	-	A/W
Responsivity @1.3μm	3.1×10^4	4.2×10^4	-	V/W
@1.55μm	3.6×10^4	5.0×10^4	-	V/W
Noise Equivalent Power (NEP):				
(100KHz f fo/2) @1.3μm	-	1.4	2.6	$pW/\sqrt{Hz}$
@1.55μm	-	1.2	2.2	$pW/\sqrt{Hz}$
Output Spectral Noise Voltage Density				
(f=100KHz-fo, Δf=1.0Hz)	-	60	80	$nV/\sqrt{Hz}$
Sensitivity (Pavg.@10^{-9}B.E.R.)@1.3μm	-42	-43	-	dBm
@1.55μm	-43	-44	-	dBm
Output Impedance		20	40	Ω
System Bandwidth, fo (3dB point)	55	70	-	MHz
Rise Time (10% to 90%)	-	5	6.4	ns
Fall Time (90% to 10%)	-	5	6.4	ns
Dynamic Range (optical)	18	20	-	dB
Output Offset Voltage	-0.7	-1.5	-3.0	V
Supply Current, +5.2V.	-	25	35	mA
-5.2V.	-	10	15	mA
Detector Leakage Current, -5.2V.	-	10	30	nA
Detector Capacitance, -5.2V.	-	0.5	-	pF
Transimpedance Resistor	-	100	-	kΩ

At an ambient temperature (T_A) of 22°C, negative photodiode bias of -5.2VDC, preamplifier operating voltages of +5.2VDC and -5.2VDC, and the signal output AC (capacitively) coupled.

S/N: 0098 TEST SUPERVISOR: [signature] DATE: Jan 28/89

CD: _____ Q.C.: _____ DATE: _____

Measured Values

Responsivity @1.3μm	3.8×10^4	V/W into 50Ω
" "	6.1×10^4	V/W into 1000Ω
Detector Leakage Current @5.2V	15.0	nA
Supply Current, +5.2V	24	mA
" " -5.2V	3.5	mA
Output Offset Voltage	-2.62	V
Output Impedance	40	Ω
System Bandwidth, fo (3dB point)	67	MHz into 50Ω
System Bandwidth "	73	MHz into 1000Ω
Output Spectral Noise Voltage Density (AVG)	44	$nv/\sqrt{Hz}$ into 50Ω
" " " " " (Peak)	70	" " "

C30986 Series

S/N: 0098 TEST SUPERVISOR: JC DATE: Juin 28/84

CD: _____ Q.C.: _____ DATE: _____

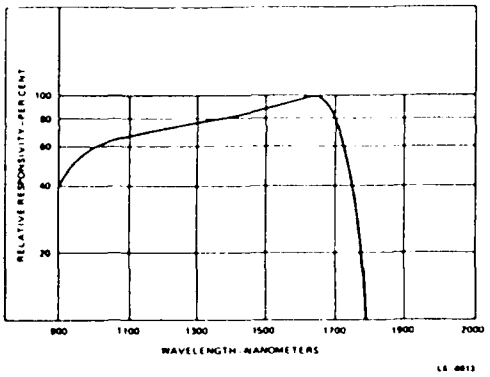

- Typical Spectral Responsivity Characteristic

- Dimensional Outline -

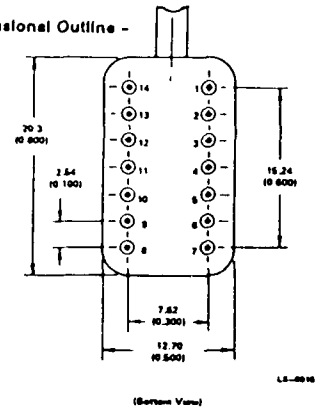

Dimensions in millimeters. Dimensions in parentheses are in inches.

Pin Connections

1: Negative Bias for Photodiode
2, 6, 9, 11, 12, 13, 14: No Connection, Do Not Use
3, 5, 8: Ground (Case and Power Supply)
4: $-V_{cc}$ Negative Bias for Amplifier
7: Signal Output
10: $+V_{cc}$ Positive Bias for Amplifier

2dB/div

20nV/Hz$^{1/2}$ /div

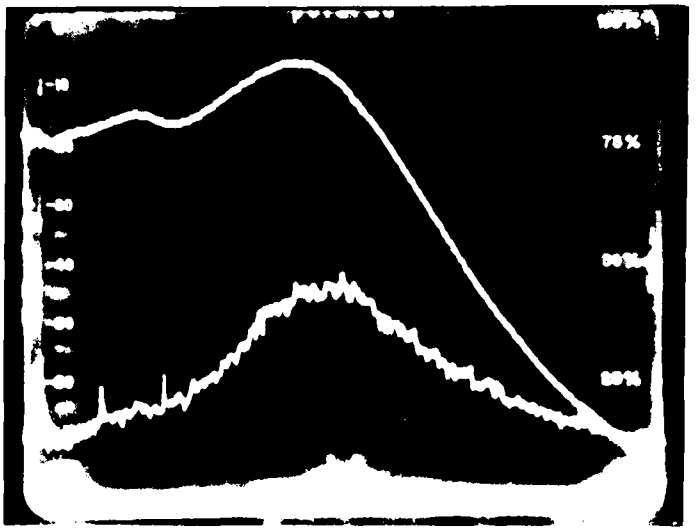

o/p Load: 50 ohms

C30986 Series

Electrical Characteristics C30986-70QC-01

	Min.	Typ.	Max.	Units
Detector Responsivity (coupled) @1.3μm	.57	.66	-	A/W
@1.55μm	.68	.79	-	A/W
Responsivity @1.3μm	3.1×10^4	4.2×10^4	-	V/W
@1.55μm	3.6×10^4	5.0×10^4	-	V/W
Noise Equivalent Power (NEP):				
(100KHz f fo/2) @1.3μm	-	1.4	2.6	$pW/\sqrt{Hz}$
@1.55μm	-	1.2	2.2	$pW/\sqrt{Hz}$
Output Spectral Noise Voltage Density				
(f=100KHz-fo, Δf=1.0Hz)	-	60	80	$nV/\sqrt{Hz}$
Sensitivity (Pavg.@10^{-9}B.E.R.)@1.3μm	-42	-43	-	dBm
@1.55μm	-43	-44	-	dBm
Output Impedance		20	40	Ω
System Bandwidth, fo (3dB point)	55	70	-	MHz
Rise Time (10% to 90%)	-	5	6.4	ns
Fall Time (90% to 10%)	-	5	6.4	ns
Dynamic Range (optical)	18	20	-	dB
Output Offset Voltage	-0.7	-1.5	-3.0	V
Supply Current, +5.2V.	-	25	35	mA
-5.2V.	-	10	15	mA
Detector Leakage Current, -5.2V.	-	10	30	nA
Detector Capacitance, -5.2V.	-	0.5	-	pF
Transimpedance Resistor	-	100	-	kΩ

At an ambient temperature (T_A) of 22°C, negative photodiode bias of -5.2VDC, preamplifier operating voltages of +5.2VDC and -5.2VDC, and the signal output AC (capacitively) coupled.

S/N: 0097 TEST SUPERVISOR: [signature] DATE: Jan 28/88

CD: _____ Q.C.: _____ DATE: _____

Measured Values

Responsivity @1.3μm	3.7×10^4	V/W into 50Ω
" "	7.4×10^4	V/W into 1000Ω
Detector Leakage Current @5.2V	7.0	mA
Supply Current, +5.2V	29	mA
" " -5.2V	3.8	nA
Output Offset Voltage	-2.52	V
Output Impedance	49	Ω
System Bandwidth, fo (3dB point)	65	MHz into 50Ω
System Bandwidth "	73	MHz into 1000Ω
Output Spectral Noise Voltage Density (AVG)	44	$nv/\sqrt{Hz}$ into 50Ω
" " " " " (Peak)	68	" " "

C30986 Series _____

S/N: 0097 TEST SUPERVISOR: FC DATE: Juin 28/89

CD: _____ Q.C.: _____ DATE: _____

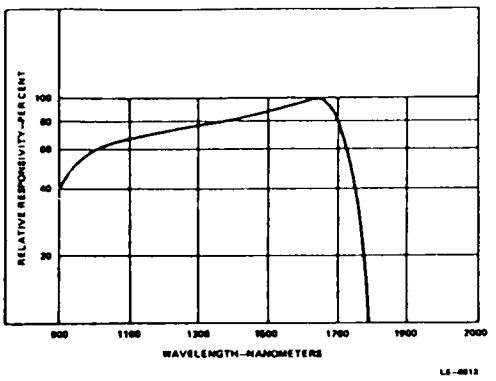

- Typical Spectral Responsivity Characteristic

- Dimensional Outline -

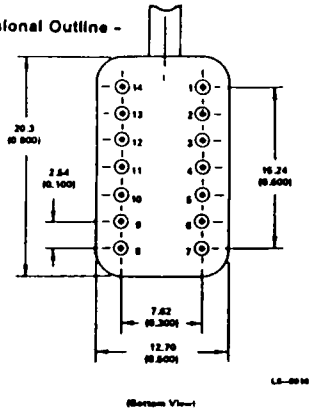

Dimensions in millimeters. Dimensions in parentheses are in inches.

Pin Connections

1: Negative Bias for Photodiode
2, 6, 9, 11, 12, 13, 14: No Connection, Do Not Use
3, 5, 8: Ground (Case and Power Supply)
4: $-V_{cc}$ Negative Bias for Amplifier
7: Signal Output
10: $+V_{cc}$ Positive Bias for Amplifier

2dB/div

20nV/Hz $^{1}/_{2}$ /div

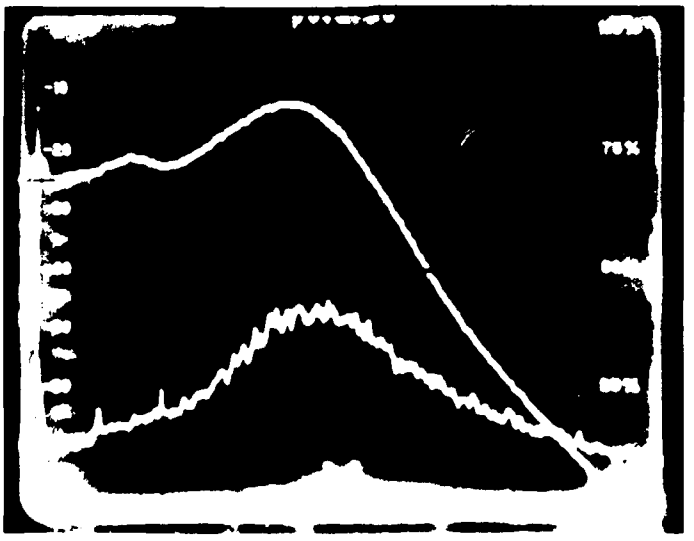

o/p Load: 50 ohms

C30986 Series

Electrical Characteristics C30986-70QC-01

	Min.	Typ.	Max.	Units
Detector Responsivity (coupled) @1.3μm	.57	.66	-	A/W
@1.55μm	.68	.79	-	A/W
Responsivity @1.3μm	$3.1x10^4$	$4.2x10^4$	-	V/W
@1.55μm	$3.6x10^4$	$5.0x10^4$	-	V/W
Noise Equivalent Power (NEP):				
(100KHz f fo/2) @1.3μm	-	1.4	2.6	pW/√Hz
@1.55μm	-	1.2	2.2	pW/√Hz
Output Spectral Noise Voltage Density				
(f=100KHz-fo, Δf=1.0Hz)	-	60	80	nV/√Hz
Sensitivity (Pavg.@10^{-9}B.E.R.)@1.3μm	-42	-43	-	dBm
@1.55μm	-43	-44	-	dBm
Output Impedance		20	40	Ω
System Bandwidth, fo (3dB point)	55	70	-	MHz
Rise Time (10% to 90%)	-	5	6.4	ns
Fall Time (90% to 10%)	-	5	6.4	ns
Dynamic Range (optical)	18	20	-	dB
Output Offset Voltage	-0.7	-1.5	-3.0	V
Supply Current, +5.2V.	-	25	35	mA
-5.2V.	-	10	15	mA
Detector Leakage Current, -5.2V.	-	10	30	nA
Detector Capacitance, -5.2V.	-	0.5	-	pF
Transimpedance Resistor	-	100	-	kΩ

At an ambient temperature (T_A) of 22°C, negative photodiode bias of -5.2VDC, preamplifier operating voltages of +5.2VDC and -5.2VDC, and the signal output AC (capacitively) coupled.

S/N: 0095 TEST SUPERVISOR: L Colclough DATE: June 28/89

CD: _____ Q.C.: _____ DATE: _____

Measured Values

Responsivity @1.3μm	$3.9x10^4$	V/W into 50Ω
" "	$7.1x10^4$	V/W into 1000Ω
Detector Leakage Current @5.2V	8.0	nA
Supply Current, +5.2V	240	mA
" " -5.2V	3.6	mA
Output Offset Voltage	-2.71	V
Output Impedance	41	Ω
System Bandwidth, fo (3dB point)	65	MHz into 50Ω
System Bandwidth "	72	MHz into 1000Ω
Output Spectral Noise Voltage Density (AVG)	90	nv/√Hz into 50Ω
" " " " " (Peak)	70	" " "

C30986 Series

S/N: 0095 TEST SUPERVISOR: JP DATE: Juin 28/89

CD: _____ Q.C.: _____ DATE: _____

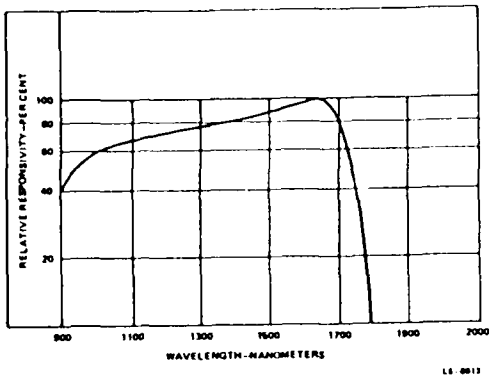

- Typical Spectral Responsivity Characteristic

- Dimensional Outline -

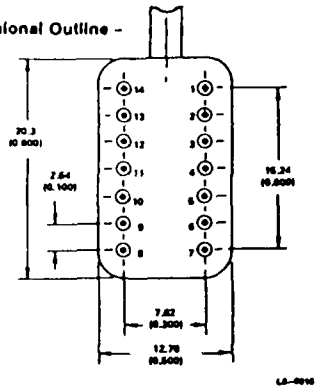

Dimensions in millimeters. Dimensions in parentheses are in inches.

Pin Connections

1: Negative Bias for Photodiode
2, 6, 9, 11, 12, 13, 14: No Connection, Do Not Use
3, 5, 8: Ground (Case and Power Supply)
4: $-V_{cc}$ Negative Bias for Amplifier
7: Signal Output
10: $+V_{cc}$ Positive Bias for Amplifier

2dB/div

20nV/Hz$^{1/2}$ /div

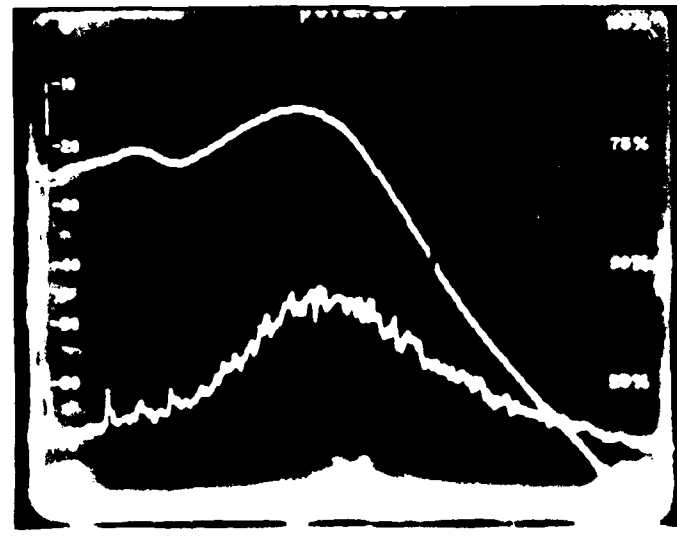

o/p Load: 50 ohms

C30986 Series

Electrical Characteristics C30986-70QC-01

	Min.	Typ.	Max.	Units
Detector Responsivity (coupled) @1.3μm	.57	.66	-	A/W
@1.55μm	.68	.79	-	A/W
Responsivity @1.3μm	3.1×10^4	4.2×10^4	-	V/W
@1.55μm	3.6×10^4	5.0×10^4	-	V/W
Noise Equivalent Power (NEP):				
(100KHz f fo/2) @1.3μm	-	1.4	2.6	$pW/\sqrt{Hz}$
@1.55μm	-	1.2	2.2	$pW/\sqrt{Hz}$
Output Spectral Noise Voltage Density				
(f=100KHz-fo, Δf=1.0Hz)	-	60	80	$nV/\sqrt{Hz}$
Sensitivity (Pavg.@10^{-9}B.E.R.)@1.3μm	-42	-43	-	dBm
@1.55μm	-43	-44	-	dBm
Output Impedance		20	40	Ω
System Bandwidth, fo (3dB point)	55	70	-	MHz
Rise Time (10% to 90%)	-	5	6.4	ns
Fall Time (90% to 10%)	-	5	6.4	ns
Dynamic Range (optical)	18	20	-	dB
Output Offset Voltage	-0.7	-1.5	-3.0	V
Supply Current, +5.2V.	-	25	35	mA
-5.2V.	-	10	15	mA
Detector Leakage Current, -5.2V.	-	10	30	nA
Detector Capacitance, -5.2V.	-	0.5	-	pF
Transimpedance Resistor	-	100	-	kΩ

At an ambient temperature (T_A) of 22°C, negative photodiode bias of -5.2VDC, preamplifier operating voltages of +5.2VDC and -5.2VDC, and the signal output AC (capacitively) coupled.

S/N: 0094 TEST SUPERVISOR: L Celata DATE: Jan 28/89

CD: _____ Q.C.: _____ DATE: _____

Measured Values

Responsivity @1.3μm	8.4×10^4	V/W into 50Ω
" "	6.7×10^4	V/W into 1000Ω
Detector Leakage Current @5.2V	5.0	nA
Supply Current, +5.2V	24	mA
" " -5.2V	4.5	mA
Output Offset Voltage	-2.48	V
Output Impedance	48	Ω
System Bandwidth, fo (3dB point)	65	MHz into 50Ω
System Bandwidth "	73	MHz into 1000Ω
Output Spectral Noise Voltage Density (AVG)	41	$nv/\sqrt{Hz}$ into 50Ω
" " " " " (Peak)	64	" " "

C30986 Series

S/N: 2014 TEST SUPERVISOR: [illegible] DATE: June 28/84

CD: _____ Q.C.: _____ DATE: _____

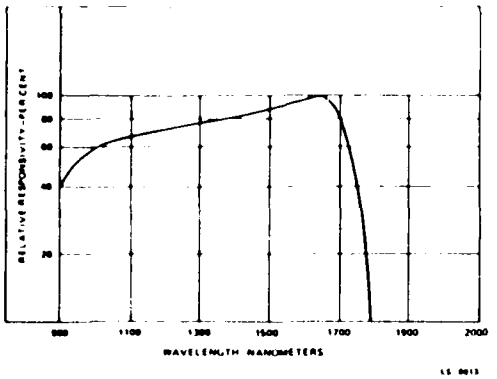

- Typical Spectral Responsivity Characteristic

- Dimensional Outline -

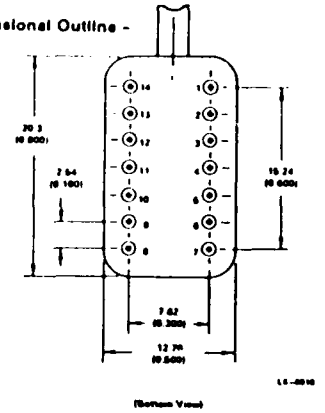

Dimensions in millimeters. Dimensions in parentheses are in inches.

Pin Connections

1: Negative Bias for Photodiode
2, 6, 9, 11, 12, 13, 14: No Connection, Do Not Use
3, 5, 8: Ground (Case and Power Supply)
4: $-V_{cc}$ Negative Bias for Amplifier
7: Signal Output
10: $+V_{cc}$ Positive Bias for Amplifier

2dB/div

20nV/Hz $^{1}/_{2}$ /div

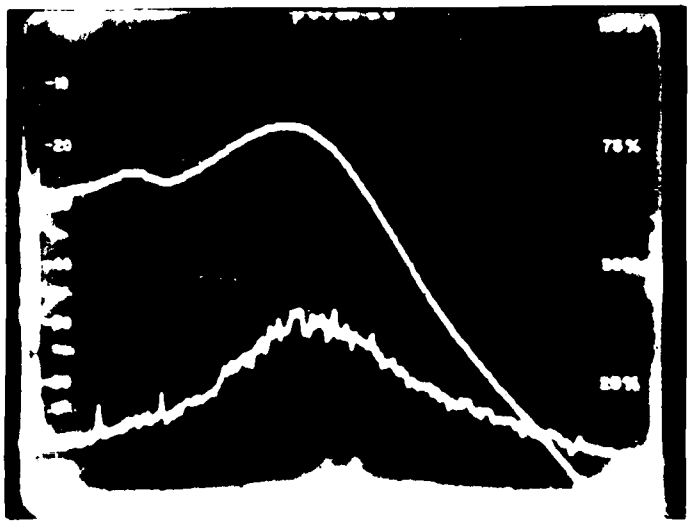

o/p Load: 50 ohms

APPENDIX C

MEASURED DATA ON 5 PIN-FET RECEIVERS SUPPLIED AS PART OF THE REQUIREMENTS OF THIS CONTRACT

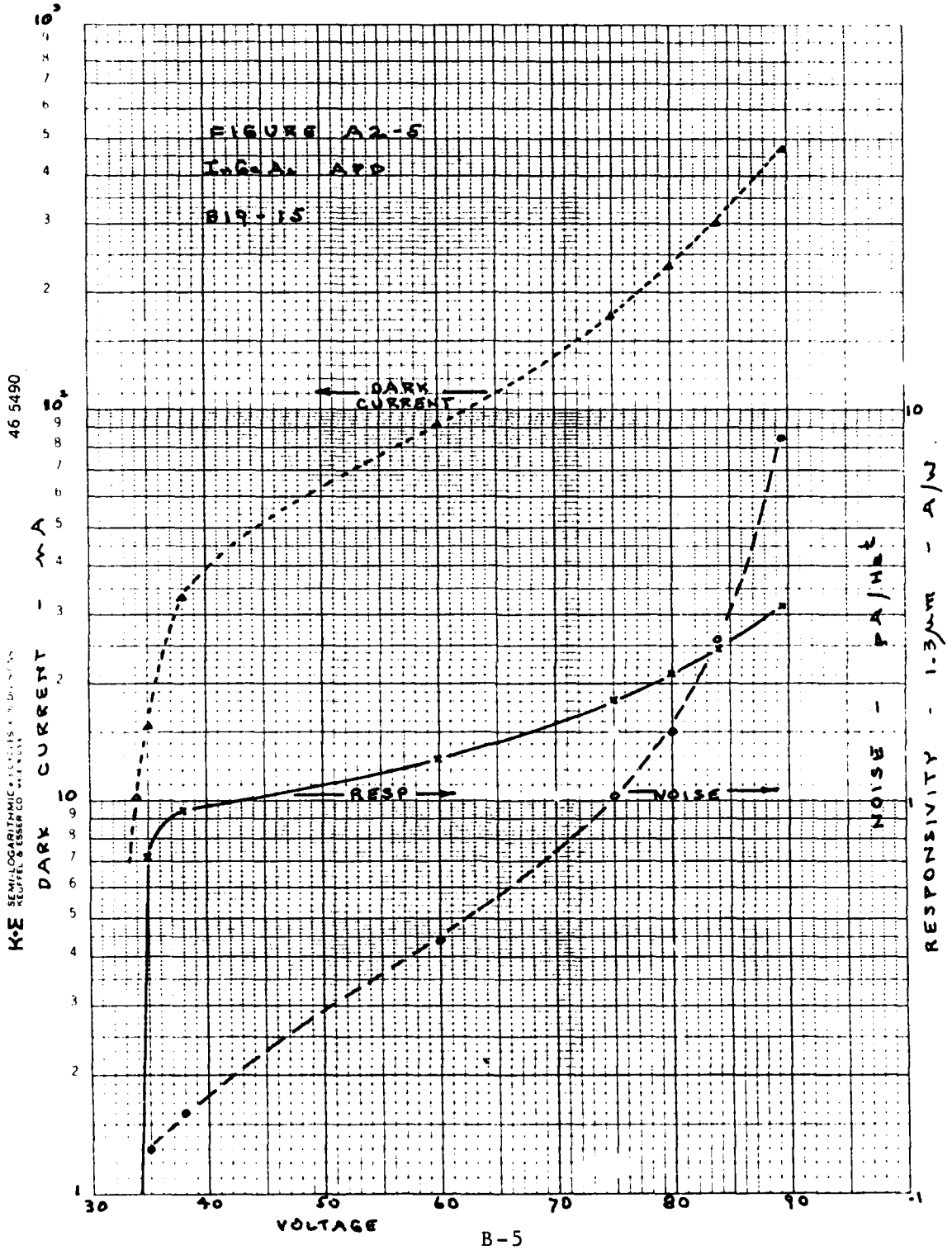
FIGURE A2-5
InGaAs APD
B19-15
DARK CURRENT
RESP
NOISE
DARK CURRENT - MA
NOISE - PA/Hz½
RESPONSIVITY - 1.3μm - A/W
VOLTAGE
30
40
50
60
70
80
90
46 5490
K·E SEMI-LOGARITHMIC
KEUFFEL & ESSER CO.

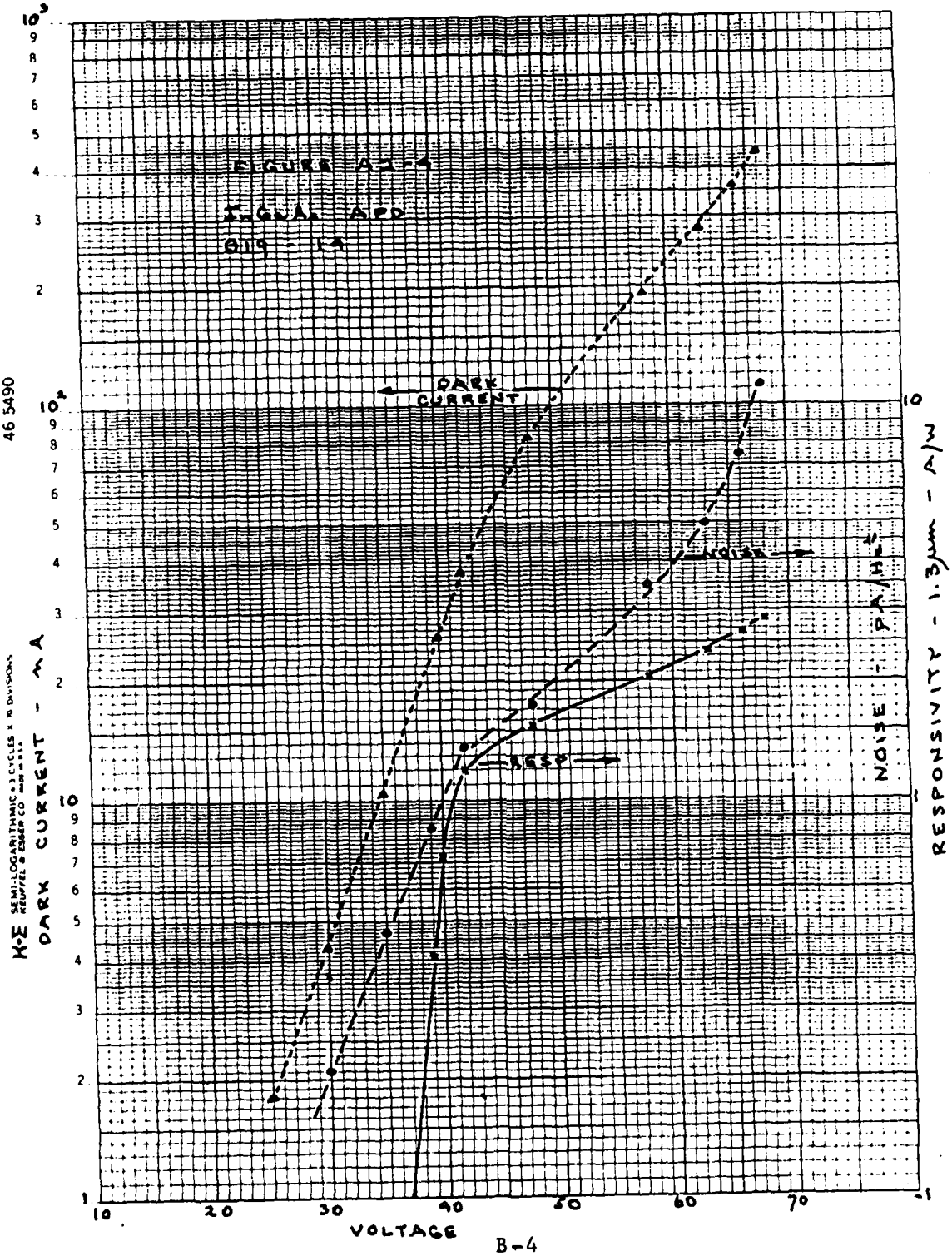
FIGURE A-4
I-GaAs APD
0119 - 14
46 5490
K+E SEMI-LOGARITHMIC 3 CYCLES X 10 DIVISIONS
DARK CURRENT - μA
DARK CURRENT
NOISE
RESP
NOISE - PA/Hz^½
RESPONSIVITY - 1.3μm - A/W
VOLTAGE
10
20
30
40
50
60
70

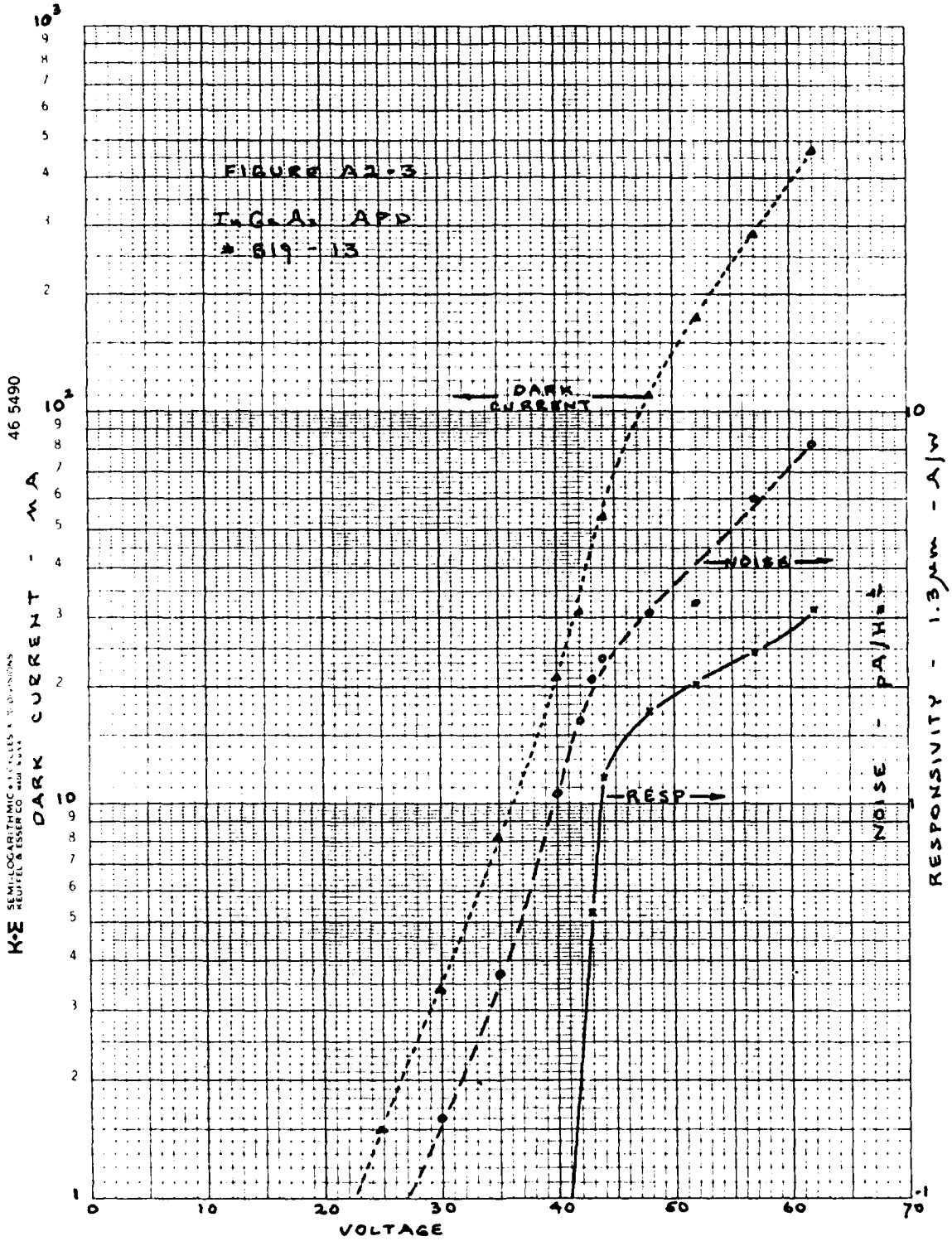
FIGURE A2-3
I.G.A. APD
619 - 13
DARK CURRENT
NOISE
RESP
DARK CURRENT - MA
RESPONSIVITY - 1.3μm - A/W
NOISE - pA/Hz^½
VOLTAGE
0
10
20
30
40
50
60
70
46 5490
K·E SEMI-LOGARITHMIC

MISSION
of
Rome Air Development Center

RADC plans and executes research, development, test and selected acquisition programs in support of Command, Control Communications and Intelligence (C^3I) activities. Technical and engineering support within areas of technical competence is provided to ESD Program Offices (POs) and other ESD elements. The principal technical mission areas are communications, electromagnetic guidance and control, surveillance of ground and aerospace objects, intelligence data collection and handl..g, information system technology, solid state sciences, electromagnetics and electronic reliability, maintainability and compatibility.

Printed by
United States Air Force
Hanscom AFB, Mass. 01731

END

FILMED

6-85

DTIC